AMAART

Active and Monitoring **Ma**terials for the Environmentally Safe Storage and Exhibition of Works of **Art**

Facoltà di Scienze Matematiche, Fisiche e Naturali

Dipartimento di Scienze della Terra

Scuola di dottorato "Vito Volterra" in Scienze Astronomiche, Chimiche, Fisiche, Matematiche e della Terra

Maria Paola Staccioli

Matricola 1096546

Docente guida
Coordinatore

Dott.ssa Gabriella Di Carlo

Prof. Silvio Mollo

Prof. Gabriele Favero

Prof.ssa Anna Maria Siani

A.A. 2022-2023

Summary of contents

Abstract

The impact of atmospheric pollutants such as volatile organic compounds (VOCs) in corrupting and deteriorating different classes of works of art is of global concern. Indoor pollutants can be off gassed by different building materials, including items of the collection and display and storage cases. Granting the optimal environmental conditions around the art objects helps to minimize the pollutants amount in the microclimate within the storage items, eliminating the need for periodical direct interventions on the works of art. To mitigate the pollutant concentration in museum indoor environment, passive absorbers can be considered as the most suitable system to be adopted, since the number of items exposed and stored makes the use of active devices too complex and expensive. Nowadays, the substances commercially available for the removal of VOCs materials have some drawbacks that should be taken into account, such as cost, mitigation obtained purely by physisorption and poor sustainability. In this Phd research project, performed in the CNR-ISMN Research Group within the H2020 APACHE "Active & intelligent PAckaging materials and display cases as a tool for preventive conservation of Cultural Heritage" Project (GA n. 814496), chitosan-based aerogels were designed and produced to give a solid tool for VOCs mitigation in museum environments. Chitosan was used for the development of VOCs absorbers thanks to its numerous advantages, namely cost effectiveness, biocompatibility, abundance and adsorption efficiency. Different kind of aerogels were produced changing the dissolution agents, the amount of chitosan in the starting solution to be freeze dried and the fillers added to enhance the adsorption capacity and the antifungal properties. The aerogels thus produced were characterized by means of FE-SEM to study their porosity and structure. The adsorption efficiency of the aerogels towards certain pollutants was then checked by

weight gain in tailored polluted environments, following a procedure of adsorption and desorption. A characterization by means of ATR-FTIR spectroscopy of the aerogels was carried out before and after their exposure to some pollutants, in order to check the chemical interaction of the chitosan and the fillers with the pollutants. The analysis of the mitigation efficacy of the aerogels continued using metal coupons as markers of the air-quality in polluted environment, in the presence of the developed aerogels. The results obtained from this research are promising, since most of the aerogels showed a good structure, a good porosity and an efficient mitigation power. As regards the tests in polluted environments, chitosan formulations were optimized and functionalised with C.C., since a good physisorption of the pollutants was observed and the chemisorption by chitosan and C.C. of different class of pollutants was detected. Also, the mitigation of the pollutants by the aerogels observed analysing the corrosion products on the metal coupons gave clues of the efficacy of the selected system. Some of the aerogels obtained from the selected formulation are now exposed in real environments.

In parallel with the study and the development of the chitosan-based aerogels, the chemical, morphological and structural properties of the sensing materials developed by the CNR-ISM and the CNR-ISMN Research Groups- within the APACHE Project - for the development of a multisensor able to detect some pollutants in museum environments were investigated during their development and after the tests in polluted environments. The analysis of the metal tracks' surface of the sensors helped to understand the results obtained by the CNR-ISM, by means of impedance spectroscopy analysis carried out during the exposure of the sensors in tailored polluted environments. In the CNR-ISMN Research Group, the metal tracks were

characterized to understand the surface modifications after exposure of the sensors in tailored polluted environments.

1 Introduction

The impact of atmospheric pollutants such as volatile organic compounds (VOCs) in corrupting and deteriorating different classes of works of art is of global concern. In most situations, indoor-generated pollutants pose a greater risk to collections than outdoor-generated pollutants. Typically, this is because the indoor source is in close and continuous proximity to the objects. Cultural heritage objects are frequently stored in unsuitable climate conditions, both in exhibition hall and in museums warehouses. The pollutants present in storage/display box microclimates significantly accelerate degradation and make objects materials lose their aesthetics and significance. Indoor pollutants are usually generated within the building. They can be off gassed by different building materials including items of the collection and display and storage cases. Granting the optimal environmental conditions around the art objects helps to minimize the pollutants amount in the microclimate within the storage items eliminating the need for periodical direct interventions on the works of art. Indirect measures and actions are thus very important since there is no contact at all with the materials and structures of the items. For a correct conservation of

the art works, the so-called Preventive Conservation (PC) entails the monitoring and adjusting of the museum environments, according to some limits agreed. The prevention of degradation is a very important issue to deal with since, in the long term, PC is more cost efficient than remedial conservation, which can be incredibly more expensive than appropriate PC measures and that is, often, unenforceable. It is therefore important, where necessary, to mitigate the concentration of the most dangerous pollutants. The monitoring of dangerous species concentration in indoor museum environment is necessary to check the quality of the air and assess whether or not to take action. The pollution monitoring tools designed for human safety applications can be used in museum environments but do have some important limitations. Art objects can visibly react to very low pollutant concentration, lower than that typically measured to assess a safe environment for human beings. Furthermore, since the market is focused on the purification of the indoor air from the pollutants affecting human health, targeted tools for the monitoring and the mitigation of the most dangerous pollutants for art objects are not yet available.

Within the PhD Research Project AMAART, new materials were developed and studied to mitigate the concentration of some of the most dangerous pollutants for the objects kept in storage and exhibition environments. The materials so developed were characterized and tested so as to obtain a final product with specific features such as biocompatibility, cost effectiveness, ease of use and adsorption efficacy. This activity was carried out in the CNR-ISMN Research Group (Institute for the Study of Nanostructured Materials of the National Research Council of Italy) in the framework of the H2020 Project APACHE (Active & intelligent PAckaging materials and display cases as a tool for preventive conservation of Cultural Heritage –

Grant Agreement N. 814496, started on 01/01/2019, duration 42 months, http://www.apacheproject.eu/).

The CNR-ISM (Consiglio Nazionale delle Ricerche – Istituto di Struttura della Materia) contributed, within the H2020 Project APACHE, to the development of a Smart Active Multisensor for the detection of environmental pollutants. Within this PhD, performed at CNR-ISMN in the framework of the APACHE project, the chemical-physical characterization of the sensors, during their setup and after the application tests of the device, was carried out.

1.1 Indoor pollutants

The chemical species that could alter the chemical, physical and structural nature of a cultural heritage artefact were first identified and an insight of their aggressiveness towards various materials was then provided.

1.2 Sources

The most common indoor-generated gases that pose a serious threat to cultural property are acetic acid (CH_3COOH), formic acid (HCOOH), acetaldehyde (CH_3CHO), formaldehyde (HCHO), hydrogen sulfide (H_2S), nitrogen oxides (NO_x), sulfur dioxide (SO_2) and ozone (O_3) [1][2][3][4] [5]. Inside the museums' premises, these pollutants can be off-gassed from paints, lacquers and varnishes, wood furniture, sealants, adhesive tape, carpets, cleaners, insecticides, fungicides as well as many other materials, products and also devices [6].

Organic acids are off-gassed by timber, paints, adhesives, varnishes and sealants meanwhile aldehydes are released by timber, adhesives, varnishes and paints [6] [7]. The water-soluble property of phenol formaldehyde and urea formaldehyde resins and glues used as bonding agent in furniture made of particleboards, makes these resins and glues be the most important and continuous sources of aldehydes in dwellings [8]. Formaldehyde can be, in fact, emitted as free formaldehyde or as product of resin or glue hydrolysis. In their study, Baez et al. (2002) [9] measured values of carbonyl concentration in indoor air higher than in outdoor air for seven sampling sites (houses, museums, offices) and, more in general, they observed a ratio of 1 to 5 of outdoor carbonyls concentration in relation to carbonyls indoor concentrations, thus corroborating the existence of various indoor carbonyls sources. A similar study was conducted by Marchand at al. (2006) [10] who observed an indoor/outdoor air concentrations ratio of both formaldehyde and acetaldehyde of about 10 and 7.3, respectively. In literature, volatile organic compounds emission in buildings has been divided into primary and secondary emission. Primary emission belongs to non-bound Volatile Organic Compounds (VOCs) from, e.g., additives, antioxidants, monomers, plasticizers, solvents and unreacted raw materials. Secondary emission belongs to originally chemically or physically bound VOCs (VOCs that are emitted or formed by different mechanisms, e.g. decomposition, hydrolysis, oxidation, and adsorption processes on the material surface) [11]. For some products, secondary emission can last much longer than primary emission that usually decay within a year. An example of long lasting secondary emission comes from linoleum, a floor covering made of linseed oil, pine resin, cork dust, wood flour and mineral fillers. During the drying of linseed oil, an

oxidation and polymerization process takes place, during which the triglycerides undergo cross-linking [12] and a considerable uptake of oxygen occurs so that the oil gains up to 40% of its original weight. Some of its weight is then lost during the oxidation reactions which originate from the oxidative cleaving of double bonds in the fatty acids chains and result in the decomposition and loss of volatile compounds that are mainly aldehydes and carboxylic acids [11][13]. Furthermore, as far as secondary emission processes are concerned, H. Wang et al. (2006) studied the ozone influence in the oxidative processes that induce emission of aldehydes on indoor surfaces in various sampling sites and stated that, no matter what the materials present in a site are, daily use of consumer products, including oils and cleaners, appear to regenerate the surfaces, continuously supplying unsaturated fatty acids or triglycerides [12]. The reaction of ozone with VOCs having unsaturated carbon-carbon (C=C) bonds is considered to be mainly responsible for the indoor chemical formation of aldehydes. Zhang et al. (1994) observed in their study that the concentration of acetaldehyde and of other aldehydes dangerous for human health were significantly correlated to ozone [14]. Also formaldehyde was found to have a significant formation via ozone chemistry but, since this aldehyde has various strong direct emission sources (as already shown), its concentration is poorly correlated with indoor ozone compared to acetaldehyde [14] whose major primary indoor source comes from human metabolism as it is present in human expired air [15]. In the literature, clues regarding the formation of organic acids in addition to aldehydes via ozone reaction with unsaturated VOCs were also shown, assuming a biradical reaction with water as a catalyst corroborated by the HCOOH-humidity relationship observed [16]. Furthermore, Zhang et al. (1994) [16] proposed the participation of the

nitrate radical NO_3 in the indoor conversion process from HCHO to HCOOH, after they observed a markedly higher rate of formic acid formation in presence of NO_2, O_3 and formaldehyde than when only O_3 and formaldehyde are present. Organic acids, as acetic acid and formic acid, can be directly produced by wooden construction materials as well as by the oxidation of their aldehydic counterpart. The amount of their emission depends, among others, on the type of wood; some hardwoods give a high emission of acetic acid that is formed from the hydrolyses of acetyl groups in hemicellulose [17].

Sulfur compounds are mostly of natural origin and have few indoor sources. The main outdoor sources of hydrogen sulfide (H_2S) are marine biological activity and active volcanoes (H_2S reacts rapidly with oxygen and forms both SO_2 and H_2SO_4) whereas sulfur dioxide (SO_2) is mainly produced anthropically by combustion of sulfur containing fossil fuels, including coal, gasoline, petroleum and diesel fuel (on combustion the sulfur in the fuel is converted almost quantitatively to sulfur dioxide), by pulp and paper production, by the cement industry and by petroleum refineries where less expensive, higher-sulfur-content fuels are used, and in other activities such as metal smelting, biomass combustion and agricultural waste burning [1] [18]. Since, nowadays, in developed countries, much of the sulfur is removed from motor fuels in the refining process and from stack gases prior to the emission, the less volatile fraction of crude oil and hence shipping which burns residual fuel oil is considered the first emitter of sulfur dioxide [19]. Indoor, sulfur dioxide can be produced by sulfur-containing fuels or firewood that are used to cook and heat, by vulcanized rubber or by propane- or gasoline-powered machines, equipment, and generator [1]. As regards reduced sulfur gases as hydrogen sulfide present indoor, they can

be emitted by wool and from people by a variety of mechanisms. These compounds are generated in the oral cavity as a result of microbial metabolism and they are also produced in the gut [20]. In addition, as just mentioned, reduced sulfur gases can be released by wool, especially if under UV or even sunlight irradiation or when it is hot (50°C), through the thermal or photochemical degradation of its cystine-containing protein [21]. The amount of indoor sulfur pollutants thus largely depends on the kinds and intensity of indoor activities and the efficiency of air-exchange and ventilation systems.

As stated by Gilbert et al. (2006) in their study about the indoor concentration of nitrogen oxide and formaldehyde [22], in contrast to formaldehyde, indoor concentrations of nitrogen dioxide (NO_2) result positively correlated with air change rates because of the significant contribution of outdoor sources to indoor levels. This pollutant, in fact, is a secondary pollutant resulting from the oxidation in the air by available oxidant (particularly ozone) of nitrogen oxide (NO) whose main sources of emissions are combustion processes; fossil fuel power stations, motor vehicles and domestic combustion appliances emit nitrogen oxides, mostly in the form of nitric oxide (NO) and some (usually less than about 10%) in the form of nitrogen dioxide (NO_2) [22]. Furthermore oxidation (by ozone, UV irradiation, etc.) of nitrogen oxides can occur both indoors and outdoors with generation of very highly reactive species as nitrous acid (HNO_2) and nitric acid (HNO_3). The indoor production of NO_2 is associated with the presence of combustion appliances such as gas stoves [23] and dry-process photocopiers [24].

Ozone (O_3) is a major constituent of smog that directly affects people, plants and property. About 90% of atmospheric ozone is present in the

stratosphere and only 10% is present in the troposphere [25]. Tropospheric (ground-level) ozone is a major secondary pollutant of vehicular and industrial emissions; its formation is catalyzed by nitrogen oxides (NOx = NO + NO_2), often emitted simultaneously with hydrocarbons and carbon monoxide, by man-made sources [24]. Ozone natural emissions are also important, especially those related to lightning NO production and NO soil emissions. As regards indoor ozone production, laser printers are potential sources since office equipment that uses high voltage or ultraviolet light can generate it [26].

1.3 Pollutants related danger

1.3.1 *Organic pollutants (acids and aldehydes)*

In the literature, various evidences have been found about the corrosion power of carbonyl-rich environment containing formaldehyde, acetaldehyde, formic and acetic acids frequently found in display or storage settings.

The way aldehydes could damage art materials is far from clear and seems to require oxidation. The analysis carried out in different studies concerning the most ordinary organic pollutants damage action in museums, revealed a connection between aldehyde aggressive power towards different materials and the presence of oxidant species and light, suggesting that oxidation is an important control on corrosion [1] [27] [28]. According to this theory, aldehydes are oxidized through photochemical or radically induced oxidation. The hydrogen atom next to the carbonyl carbon can be extracted in oxidation and replaced by an oxygen or a hydroxyl group. An aldehyde can be thus transformed into organic acid, the organic acid then

attacks the museum object chemically, losing its hydrogen in the process and leaving behind its anion (e.g., formate or acetate) that is identified in the corrosion products [1]. Oxidants that provide the oxygen for the reaction can be strong, such as permanganate, or mild, such as hydrogen peroxide. According to M. R. Raychauduri and P. Brimblecombe (2000) [27] aldehydes are oxidized to carboxylic acids through intermediate hydrates or via Cannizzaro's reaction as well as by photochemical or radically induced oxidation. Nevertheless, D. L. A. De Faria et al. (2010), as the headline of their article [29], reassessed the role of formaldehyde in lead corrosion, stressing in their results the formation of corrosion product on Pb surfaces exposed to formaldehyde without the presence of any oxidant species. Thiago S.Puglieri et al. (2014), who investigated the effect of relative humidity (RH) and formaldehyde concentration on Pb corrosion [30], also stated that this aldehyde has an active role in Pb corrosion. In their study, S. Puglieri et al. [30] also observed that below a critical RH, no electrochemical corrosion takes place and, irrespective of the metal considered, for a clean metal surface such primary critical RH is ca. 60%. What is clear from the literature is that the reaction of organic acids and aldehydes with art materials is a contentious subject because of the high number of variables to be considered that contribute to the chemical processes. However, as regards formaldehyde, most of the studies propose that its damaging effects on art objects are correlated to the acidic forms, that is not the concentration of formaldehyde that is important, but rather its potential to oxidize to formic acid and that formaldehyde is probably less of an issue as an indoor pollutant than is often assumed [1] [27] [28] [31]. As concerns the correlation between RH values and corrosion rate, controversy exists about the role played by humidity in metal atmospheric oxidation

induced by both the aldehydes and the organic acids [30] [32]. What is commonly stated is that an increase of HR values generally involves an increase in the metal corrosion rate [30] [32] [33]. It is proven, in fact, that a thin water film on the metal surface is required for an electrochemical corrosion processes to begin and it is assumed that the thickness of such electrolyte film depends on several factors such as the relative humidity, the corroding material, the tendency of the corrosion compounds at the surface to absorb moisture and the pollutants present in the atmosphere [33]. A water adlayer (water layer adsorbed on the substrate) is ever present on metal surfaces at normal atmospheric conditions, this layer acts as a solvent for gaseous species and is where some chemical reactions can take place [34]. Hence, relative humidity is often considered a crucial parameter in determining the rate of a corrosion process. Although metals are the most sensitive materials to organic carbonyl pollutants other materials can be affected by their aggressive effects. From the results of A.-L. Dupont and J. Tétreault (2000) [35], it appears that the degradation of cellulose by exposure to acetic acid environments is dependent on the concentration of the acid and also on the aging that follows the exposure. The exposure of paper samples to 8.14 ppm of acetic acid for 40 days revealed a significant degree of degradation. A.-L. Dupont and J. Tétreault (2000) [35] thus observed a cellulose depolymerization due to acid hydrolysis, which is characterized by random chain cleavage with the cellulose fibers becoming shorter and weaker as the reaction progresses. The study also indicates that the depolymerization of the cellulose by exposure to acetic acid is more likely to occur over the long term. A subsequent study by J. Tétreault et al. (2013) [28] revealed that hydrogen peroxide and formic acid in average concentration of 30 ppm and 38 ppm, respectively, are the most reactive

volatile compounds towards cellulose with considerable damage (decrease in degree of polymerization) observed after 52 days of exposure at RH 75%. Furthermore, a considerably lower reactivity towards cellulose for acetic acid compared to that of formic acid was observed togheter with a slight alteration by aldehydes only on pre-oxidized cellulose. Actually, the co-presence of the aldehyde with its acid counterpart (acetaldehyde with acetic acid and formaldehyde with formic acid) led to a considerable inhibition of the ractivity of the acids since less damage was found in paper samples when exposed to a mixture of both the two species [28]. One hypothesis set out by the authors for the counter degradation effect of aldehydes could be a preferential weak affinity bonding. Formaldehydes and acetaldehydes may be weakly bonded near active sites on the celluose macromolecule (glycosidic bonds and hydroxyl groups) thereby limiting the access for acids, oxidants and/or water molecules, and lowering the rates of acid hydrolysys and oxidation [28]. Moreover it was observed that exposure to formaldehyde alone even seemed beneficial. This phenomenum could be explained, as shown above, by a shield action of the aldehyde towards carboxylic acids directly emitted by cellulose during its oxidation. As regards another class of materials, namely colorants, Edwin L. Williams et al. (1992) [36] studied the effects of the exposure to either formaldehyde (120 ppb concentration for 12 weeks) or pure air on water color paper of various colorants including inorganic colorants, alizarin lakes, quinacridones, triphenyl methane, indigo derivatives, arylamides and natural colorants such as curcumin. The exposure resulted in little or no color change for all the colorants tested suggesting a non-crucial role of the aldehyde in colorants' fading. O. Vilanova et al., M. Malagodi et al. and N. De Laet at al. [37] [38] [39], instead, revealed a quite important interaction between some

VOCs and inorganic pigments such as malachite and white lead whose composition is, in fact, characterized by the presence of copper and lead respectively. In particular, Marco Malagodi et al. [38] investigated the chemical modifications experienced by different historic inorganic pigments, i.e. Lead White ($PbCO_3 \cdot Pb(OH)_2$), Red Minium (Pb_3O_4), Azurite ($Cu_3(CO_3)_2(OH)_2$), and Led Tin Yellow (Pb_2SnO_4), when exposed to acetic and formic acid vapors. For each pigment studied they observed different interactions with acetic and formic acid, which induce formation of new crystalline phases and structural modifications. In each case the chemical modifications led to chromatic variations except for White Lead pigment whose reactions products' color didn't differ from the original one. Also, physicochemical alterations of gypsum were stated; after its exposure to different VOCs the loss of water molecules has been observed with the consequent generation of new crystalline phases [37]. The aggressive power of organic acids towards calcium carbonates has been noticed for many years because of the formation of salt efflorescence on porous calcareous artefacts [40]. A visible efflorescence was observed in mollusk shells and other calcareous specimens that were in storage or on display for long periods of time. This phenomenon is called Byne's Disease from the name of the naturalist who first suggested the presence of calcium acetate in the affected shells he analyzed (1899) [41]. Only three decades later it was recognized that acetic acid vapor emitted from oak wooden drawers was responsible for the formation of calcium acetate salts [42]. The same problem was observed on calcareous pottery where the presence of calcium acetate compounds was revealed and ascribed to the reaction of the calcium in the ceramic matrix with acetic acid volatiles [43] [44] [45].

The reactions between acetic and formic acids with mineral $CaCO_3$ particles was studied by M. D. King et al. (2004) [46] by means of Raman spectroscopy and optical microscopy. According to their study, reaction with formic acid produces a surface coating of formate and then the reaction appears to stop after a surface passivation. As regards acetic acid, instead, its reaction with $CaCO_3$ produces separate crystals and slowly continues over several hours. Neither reaction appeared to lead to deliquescence.
VOCs showed to be aggressive also toward glass; in various studies [47] [48] [49] [50], the white deposits observed on glass surface in sites where sources of formaldehyde and formic acid were present were analyzed and the presence of sodium formate was revealed, suggesting that the degradation is to ascribe to the reaction of formic acid, and possibly formaldehyde with sodium compounds in the glass.

1.3.2 Inorganic pollutants

In addition to organic compounds, some inorganic pollutants, among the airborne pollutants, are harmful to cultural heritage objects. We quote here: hydrogen sulphide, sulphur dioxide, nitrogen dioxide and ozone.

1.3.2.1 Hydrogen Sulphide

As regards hydrogen sulphide (H_2S), the high sensitivity of silver to tarnishing in presence of low concentration of this pollutant is well known. Thus, the atmospheric sulfidation of silver has been recognized and analyzed for a long time [51] [52] [53] [54] [55] [56] [57]; it has been assessed that H_2S concentration as low as 0.2 parts per billion (ppb) is sufficient to cause sulfidation. When copper is affected by a pollutant action, different degradation products can appear over the metal surface and, consequently, the metal can change its surface color according to the dominant reaction

product. The principal product of the reaction of HS^- and silver is silver sulfide (Ag_2S), also known as acanthite (one of three polymorphs of Ag_2S) [58] which generates a blackish patina easily distinguishable from patina composed of basic copper sulfates and chlorides that have a greenish color [59]. In the literature, there are a number of conflicting analysis results on the influence of relative humidity on the corrosion of silver when exposed to reducing sulfurous gases. Thus, the question whether a higher % RH allows for a lower critical H_2S concentration is still open [58]. Graedel et al. [56] observed a behavior of copper similar to that of silver in presence of a few ppm of H_2S. The predominant corrosion products observed in that case are copper sulfide (Cu_2S) and cuprite (Cu_2O) [56] [60].

Smith et al. (2001) [61] [62] investigated the degradation of pigments of copper and lead carbonates, oxides, hydroxides and sulphates by hydrogen sulphide. Sample pigments containing copper were all found to react rapidly to form blue–black covellite (CuS) in response to exposure to H_2S whereas most of pigments containing lead reacted quickly to form black galena (PbS). In particular the appearance after reaction with H_2S, both just after the exposition and after 5 days, was evaluated for lead white $2PbCO_3{\cdot}Pb(OH)_2$, lead (II) carbonate $PbCO_3$, lead (II) sulphate $PbSO_4$, lead (II) sulphate tribasic monohydrate $PbSO_4{\cdot}3PbO{\cdot}H_2O$, massicot PbO, malachite $CuCO_3{\cdot}Cu(OH)_2$, basic verdigris $Cu(CH_3COO)_2{\cdot}2Cu(OH)_2$, azurite $2CuCO_3{\cdot}Cu(OH)_2$, litharge PbO, red lead Pb_3O_4 or $2PbO{\cdot}PbO_2$. The less vigorous change of color observed for lead (II) carbonate and red lead was attributed to a milder reaction with the pollutant and a consequent partial transformation to galena due to the particular structure of the pigments [61].

1.3.2.2 Sulphur Dioxide and Nitrogen Dioxide

SO_2 and NO_2 are among the selected pollutants whose indoor concentration strictly depend on the air exchange rate between the inside and the outside of the building because of their mostly outdoor sources, as previously described. Their concentration in a building is indeed normally lower than outside, even when no filtration is installed [63]. For both SO_2 and NO_2 the value of relative humidity in the indoor environment is an important parameter to be considered in order to evaluate the aggressiveness of the pollutants. Sulfur dioxide can react with water vapor in the air and form both sulfurous acid (H_2SO_3) and sulfuric acid (H_2SO_4). Outdoors, in high humidity, the acidic gases coalesce into suspended droplets, or aerosols, known as acid rain, meanwhile indoor a similar reaction implies the deposition of these acidic gases on surfaces and their subsequent damage [1][64][65]. Similarly, with the presence of humidity, the nitrogen dioxide (NO_2) can easily turn into the powerful nitric acid (HNO_3) which can damage the museum objects [64][65]. Various studies were carried out over time regarding the interaction of SO_2 and NO_2 with materials depending on the environment in which they act. Their corrosion activity has been studied changing RH values and concentration as well as the presence of other pollutants in order to study possible synergic action. The effect of SO_2 on the atmospheric metal corrosion investigated over the years by various environmental studies demonstrates that SO_2 is one of the most important corrosive agents [66]. In the case of copper and its alloys, the importance of SO_2 in the atmosphere is indicated by the frequent occurrence of copper hydroxysulfates in the corrosion layer [67]. Under ambient conditions, copper is covered by a thin cuprite layer. When exposed to humidity, the cuprite is hydroxylated. The surface copper hydroxyl groups have ion-exchange properties and other surface complexes can form. The ligand

bound to the surface copper ion can weaken the bond between this surface copper ion and its immediate neighbors (trans influence) and hence promote the dissolution of the complexes, the broken bonds are immediately hydroxylated and the process carry on [67]. In his study, Vernon (1931) [68] observed a rather different corrosion rate of copper according to the RH value set in a synthetic atmosphere containing sulphur dioxide and claimed the existence of a critical humidity lying between 63% and 75%, below which relative humidity has comparatively little, and above which it has a profound effect. In their study, Oesch and Faller (1997) [69] analyzed the corrosion products generated by the interaction of different atmospheric pollutants with copper, zinc and aluminium and they concluded that sulphur dioxide plays a central role in the copper patina formation. Accoding to R. Ericsson and T. Sydberger (1977) who studied the corrosion products formed on copper exposed to humid SO_2-containing atmospheres [70], copper (II) sulphate ($CuSO_4$ $5H_2O$) is the main crystalline product of corrosion during SO_2 exposure of copper. They also observed the formation of another sulphate after the interruption of the SO_2-supply i.e. antlerite ($CuSO_4$)$2Cu(OH)_2$. The prolonged exposure, instead, led to the formation of brochanite ($CuSO_4$ $3Cu(OH)_2$). The corrosion action of SO_2 on copper can be enhanced by the presence of other species like NO_2 that resulted to oxidize SO_2. It was found that this synergism is active only a high relative humidity value (90%). During the corrosion action, acid sulfate attacks the passive film (Cu_2O) and starts an electrochemical corrosion process [71].

As regards the interaction of sulfur dioxide and zinc, Oesch and Faller (1997) [69] stated that SO_2 exceeds by far the effects of the other air pollutants in the corrosion of zinc. Qing Quet et al. (2002) [72] studied the

corrosion of zinc under various conditions observing, in particular, the influence of NaCl deposition on the corrosion of the metal in atmospheres with and without SO_2. They concluded that the co-existence of NaCl and SO_2 can accelerate the initial atmospheric corrosion of zinc. Furthermore, analyzing the FTIR spectra of the corrosion products, they assessed that the interaction of sulfur dioxide and zinc in humid air produces Zn^{2+} and SO_4^{2-} that are mobilized in acidic aqueous solution, form ion pairs and precipitate hydrated zinc sulfates upon the evaporation of the surface water film. At high humidity, the hydrated zinc sulfates can absorb water from humid air to form an aqueous solution on the surface that tends to make way for an electrochemical corrosion process. J. E. Svensson and L. G. Johansson (1996) [73] observed an inverse correlation between the SO_2-induced corrosion of zinc and temperature at a constant RH. They ascribed the inverse dependence to the formation of sparingly soluble zinc hydroxyl sulfates at higher temperature that slows down the deposition of SO_2 on the surface, whereas the thick film of $ZnSO_4$ (aq), formed on the metal surface at low temperature, seemed not to hinder the corrosion rate. As seen for copper, the combination of SO_2 and NO_2 gives rise to a strong synergistic effect as stated by J.-E. Svensson and L.-G. Johansso [74]. In particular, they observed that the presence of traces of NO_2 and O_3 accelerates the SO_2-induced corrosion of zinc in humid air and suggested that the role of these two pollutants is connected to the process of SO_2 deposition on the zinc surface: O_3 oxidizes loosely bound four-valent sulfur on the zinc surface to sulfate while NO_2 catalyzes the oxidation of SO_2 on zinc. The increased formation of sulfate and hydrogen ions on the surface thus leads to the dissolution of solid corrosion products and to an increased rate of metal dissolution [74].

SO_2 is not only dangerous for the conservation of metal artifacts but also for organic materials such as leather and paper. Leather is very vulnerable to sulphur dioxide (SO_2) that it adsorbs in high amounts. The penetration of sulphur dioxide into leather is influenced by the nature of the organic retanning process used, condensed tannins leading primarily to surface sorption [75]. Inside the material, owing to oxidants and humidity adsorbed simultaneously or already present, SO_2 is transformed into sulphuric acid. The natural deterioration of leather is characterized by several physical and chemical changes due mainly to oxidative breakdown and to hydrolysis [76] [77]. A study of the interaction between collagen (the main protein of leather) and sulphur dioxide carried out by Karim Dif et al. (2002) determined that an ionic bond is probably created between HSO_3^- (obtained by contact of SO_2 with the residual water) and the zwitterionic form of the basic site chain of an amino acid residue.

As for leather, paper tends to pick up sulphur. Copper, iron and manganese, often present as impurities, catalyze the change of sulphur dioxide into sulphur trioxide to form sulphuric acid in the presence of moisture and, not surprisingly, one of the main causes of the weakening of paper in storage is acidity [78] [79] [80] [81]. Since the conversion of SO_2 to H_2SO_4 requires moisture, RH and temperature are thus very important parameters to be considered. Paper exposed to sulphur dioxide show an increase in acidity and a color change towards dull grey [81].

Sulphur dioxide proved also to cause damage on textiles such as silk, cotton, ramie and viscose rayon [82] [83]. Acidification of the textile material due to the trapped sulphate ions causes a chemical damage and a loss in the breaking strength of the yarns [82] [83]. Since SO_2 is mainly considered an outdoor pollutant, having found that some textile fabrics exposed at

outdoor sites having equal sunlight intensity lost more strength at urban and industrial sites than at rural sites, J. B. Upham and V. S. Salvin (1975) [84] postulated atmospheric SO_2 as a possible cause and conducted tests that assessed this supposition. According to M. Nam. Kim et al. (2012) studies, 1 ppm/day SO_2 can be considered a critical level of deterioration of some textiles [82]. The interaction products of SO_2 with pigments were also studied in order to understand the degradation mechanism that leads to a colour change. A. Alebic-Juretic and D. Sekulic-Cikovic (2009) [85] showed ambient sulphur dioxide as the possible source of damage of some painting because of the excess of sulphates detected in the soiling layer film on the paintings analysed. According to A. Alebic-Juretic and D. Sekulic-Cikovic, excess of sulphates may originate either from the reaction of sulphur dioxide with calcite, already deposited on the paintings, or as the result of sulphuric acid formation via a catalytic reaction on the surface of the paintings [85]. The effect of the pollutant on wall paintings was also studied, focusing in particular on those pigments that show a strong colour change namely hematite and red-lead pigments. Maite Maguregui et al. (2011) [86] revealed the presence of sulphate compounds arising both from pigment degradation and from the binder (calcite): original hematite was found to be turned in iron (III)sulphate nonahydrate coquimbite or paracoquimbite while the plaster calcite in gypsum. The presence of sulphate compounds and the blackening of the original red hematite were explained evidencing two possible mechanisms of reaction: 1) sulphur dioxide coming from atmospheric pollution is oxidized to sulfur trioxide (SO_3), this gas dissolves in the surface moisture in the gas-liquid interface to form sulphuric acid (H_2SO_4) 2) as the sulphur dioxide oxidizes, the Fe (III) of hematite partially reduces to Fe(II), forming black magnetite, which is a mixture of both iron

oxidation states. Meanwhile, the calcite mortar reacts with the sulphurous acid, in the presence of oxygen, giving rise to the formation of gypsum. Moreover, thanks to free sulphate available in solution on the surface of the plaster, hematite may transform into Fe (III) sulphate nonahydrate [86]. A similar process was noticed also for lead pigments; Sebastien Aze et al. (2007) [87] also attributed the darkening of a red pigment combined with the presence of gypsum to chemical processes involving atmospheric sulfur dioxide. In that case red lead (Pb_3O_4- minium) transformation into mainly plattnerite [β-PbO_2] and also anglesite [$PbSO_4$] was observed and the pigment alteration was assumed to occur through the sulphation into anglesite of lead monoxide initially present in the pigment, followed by the so-called "solvolytic disproportionation" of Pb_3O_4 [88] meanwhile, the pigment transformation into plattnerite was attributed to further interactions with acidic species originating from atmospheric pollutants [87].

As regards dyes fading by SO_2, a study on thirty-four artists' colorants was carried out by Edwin L. Will et al. (1993) [89] brushing them on watercolor or cellulose paper and exposing them to two atmospheres containing different SO_2 concentration. From this study, exposure to sulfur dioxide resulted in little or no color change except for one category of colorants: the triphenylmethanes basic fuchsin, brilliant green, and pararosaniline.

As seen above, the deterioration of plaster by SO_2 leads to the formation of gypsum. Actually, sulfur dioxide is considered the main decay factor of carbonate-based stones in polluted environments, with crust formation and solubilization of the stone being the main components [90]. The formation of gypsum has been assumed to be due to the reaction of calcium carbonate with sulfur dioxide or to the absorption of sulfur dioxide in rainwater,

liquid atmospheric aerosols, or moist film supported on a stone surface, where it is oxidized to form a sulphuric acid solution that dissolves the calcium carbonate by gypsum formation [91] [92] [93].

Unlike SO_2, NO_2 turned out not to be reactive toward zinc. Svensson et al. (1993) [94] observed that the corrosion rate in four-week exposures (400 ppb, 95% RH) of zinc was only marginally higher than in the pure air experiment. On the other hand, the combination of SO_2 and NO_2 stimulated corrosion at high humidity since an increase of the deposition rate of SO_2 on zinc was detected in the presence of NO_2 [94]. The presence of NO_2 in the environment resulted relevant. In fact, in a SO_2+NO_2 environment, a strong synergistic effect was observed thanks to a NO_2 indirect participation as a catalyst of the oxidation of SO_2 to sulphate [94] [95]. The corrosion rate of silver in the NO_2 environments resulted affected by both oxygen and humidity as in the H_2S environments, even if it has been assessed that silver can be corroded without oxygen, indicating that nitrogen dioxide oxidizes silver [96] [97]. Nitrogen dioxide is thus reported to act as an oxidant to form a metal oxide and as a pH modifier since it contributes to acidification of adsorbed water layer [96]. The hydroscopic corrosion product, $AgNO_3$, allows water to be condensed on the surface, which enhances the surface mobility and increases the tarnish rate [96]. According to the copper corrosion products detected, the nitrogen oxides have a role in the metal patina formation although to a minor extent as compared to sulphur dioxide. As for zinc, at high relative humidity (> 70%), a synergism in copper corrosion between NO_2 and SO_2 was observed since the deposition rates of sulphur dioxide increases [69][71]; possibly, a combination of the kinetic impact of the sulfur dioxide with the thermodynamic impact of the nitrogen dioxide produce a more aggressive electrolyte than the electrolytes

produced by ether gas acting alone [98]. Takazawa (1985) [99] observed that the corrosion rate of aluminium, iron, nickel and copper metal in NO_2-containing atmosphere has a nearly equal value and that the corrrosion product formed on zinc, iron, and nickel surface does not accelerate the corrosion of each metal.

As regards colorants fading by NO_2, anthraquinonic colorants resulted degraded after exposure to 5 ppm of the pollutant [100] [101]. In addition, also curcumin and indigo showed a fading, the last one quite slight compared to the other three colorants considered [100]. Colour changes have been observed also for arsenic sulphide pigments such as orpiment and realgar exposed for a 12-week period to a maximum concentration of 50 ppm of NO_2 [101].

During exposure to nitrogen oxides, the molecular weight of paper resulted to decrease, indicating cellulose chain rupture. The mechanical properties of the pure cellulose samples used by Jerosch et al. (2002) to study paper degradation caused by nitrogen oxides (softwood, hardwood, cotton) [102], showed that strength decrease at the end of the treatment is certainly related to two factors: nitrogen oxides and the acid sizing of the paper and that the major fibre strength loss is consistent with a cellulose chain-breaking mechanism.

Kim et al. (2013) [103] carried out optical, chemical, and physical evaluation on silk, cotton, ramie and hemp representative of Korean traditional textiles, dyed with 5 colours, after their exposure to different NO_2 concentrations. In this study, differences in the colour garments and in the concentration of carbonyl and C-NO_2 functional groups were observed along with a weakening of the tensile strength depending on NO_3^- concentration. Increasing pollutant concentration, an enhancement of the

garments' deterioration was observed for both the samples such as and those dyed.

As regards calcareous materials, nitrogen oxides along with sulphur dioxides react directly with the carbonate stone surface by forming acids in the presence of water and oxidising agents [104]. These acids react with the stone to form salts which either crystallise out within the stonework resulting in physical damage or they are washed away resulting in a loss of material. This damage mechanism carries on at all sulphur dioxide concentrations. On the contrary, since nitrate salts are more soluble and expand less than salts of sulphate, their associated damage is results very light. According to S.W.Massey (1999) [104], in fact, correlation studies of the damage to stone materials are unlikely to pick up the effects of NO_x due to the nature of their duration and the rather transient nature of the appearance and removal of nitrates on the stone. However, M.D. King (2004) and A. Sarmiento (2008) demonstrated that by means of Raman spectroscopy it is possible to easily reveal the presence of various nitrogen species and that calcium carbonate particles react with humid HNO_3 derived from atmospheric NO_x to form a surface coating of calcium nitrates, which then uptakes water and the reactions continues until all $CaCO_3$ is consumed [46] [105].

NOx polluted air has proven to be dangerous also for bees' wax which plays an important role as a material used for conservation of cultural heritage objects. Thanks to non-isothermal DSC measurements, Vykydalová et al. (2020) [106] observed that the presence of NOx species had a significant deteriorative effect on the thermooxidative stability of bees' wax. FTIR analysis on the exposed bees wax samples revealed the extinction of ester

groups accompanied by increase in free fatty acids content corroborating what was already verified by means of non-isothermal DSC measurements.

1.3.2.3 Ozone

Ozone was recognised to be a potential corrosion accelerator in metal corrosion research. Most of the studies mainly attribute ozone action to its catalysing activity towards other pollutants present [74] [107] [108] [109]. Despite the fact that ozone corrosion action is mainly attributed to oxidise H2S, S(IV) and nitrogen species, S. Oesch and M. Faller (1997) [69] demonstrated that ozone can enhance the corrosion processes substantially on its own. According to S. Oesch and M. Faller, the high corrosion rate observed in absence of other pollutants can be attributed to the electrochemical reduction reactions of ozone or to one of its reaction products, i.e. the hydroxy radical, which is balanced by the metal dissolution. They also observed that ozone had the strongest influence on the corrosion of copper and aluminium compared to nitrogen dioxide, sulphur dioxide, nitrogen monoxide and laboratory air. However, the relevant catalyzing action of ozone on sulphur dioxide and nitrogen dioxide is not contested since several evidences were submitted in various studies. Laboratory exposures with combinations of sulphur dioxide and ozone or nitrogen dioxide and ozone illustrated that the corrosion rate of copper [69] [109] [110], zinc [74] and silver [107] greatly increases in the presence of ozone; as briefly mentioned, this is mainly attributed to the oxidation of S(IV) to S(VI) by ozone or its reaction products and the consequent production of more aggressive species such as H_2SO_4 and to the formation of HNO_3 and N_2O_5 in the gas phase by reactions of nitrogen oxides and

ozone and the subsequent adsorption of HNO_3 in the electrolyte [69][74][107][108][109].

Zakipour et al. (1995) [110] observed that when only O_3 is added to pure air, a decrease in the surface content of monovalent copper is seen, possibly because of the formation of CuO, $Cu(OH)_2$ or both by O_3, but the amount of additional oxide/hydroxide formed, compared to pure air, was too small to be quantified by cathodic reduction or weight increase measurements. Furthermore, the corrosion effect of the combination $SO_2 + O_3$ was studied and it was found to be more enhanced than the sum of the corrosion effects of the individual gas exposure, proving a synergism exists between SO_2 and O3. As regard silver corrosion by ozone, ozone alone does not react quickly with bare silver but a measurable amount of corrosion product (Ag_2O) can be generated if bare silver reacts with reactive atomic oxygen generated from the photo-dissociation of ozone [111][112]. Molecular oxygen cannot oxidise silver at ambient temperature, and the interaction with silver is mainly limited to adsorption. Hence, it was shown that fast silver corrosion requires the combined presence of UV light and ozone since the co-presence of UV and ozone is necessary the generation of atomic oxygen. The studies of the impact of RH on the corrosion process of silver by ozone shown a behaviour which is contrary to common atmospheric corrosion experience. To clarify such phenomenon, Z. Y. Chen at al. (2010) [111] suggested that atomic oxygen reacts directly with Ag in a chemisorption process of the reactive species on the silver surface under dry conditions and instead, in the presence of humidity, atomic oxygen probably reacts with water to form OH radical, which then reacts with the Ag and a chemisorption of OH radical similar to atomic oxygen occurs. Hence, the rate of chemisorption in both dry and wet conditions resulted similar. As a result of the similar initial

chemisorption in both dry and wet conditions and formation of transport barrier, the corrosion rate of bare silver in an environment of UV light, RH and ozone is thus not sensitive to the change of RH [111]. According to R. Wiesinger et al. [112] (2013), instead, the oxide formation and the corrosion rate are dependent on the RH content in the atmosphere. In particular they observed that silver is more susceptible to ozone oxidation at 50% RH than at 0% and 90% RH. These results led to a finding concerning the role of water monolayers on the metal surface; they suggested that the observed behaviour is to ascribe to the fact that 3 or more water monolayers on a surface approach bulk water property, which is the case for RH contents of ≈65% depending on the substrate. Thus at 90% RH the surface water layers might show bulk water properties, slowing down the diffusion of ozone to the metal surface and intermediate reactions of ozone in the water film. In 50% RH atmosphere, instead, 2 water monolayers should be present which is more a an adlayer system. In a dry atmosphere (0% RH), as mentioned above, molecular and atomic oxygen are chemisorbed during the first few hours of exposure, furthermore ozone directly oxidizes silver to form Ag_2O surface species [112]. In contrast to silver, zinc showed no signs of visible corrosion product after the exposure to both ozone alone at high RH values [74] and UV light irradiation [108]. Svensson et al. (1993) [74] suggested that, since O_3 and its products of decomposition do not create an electrolyte on the surface, it can only contribute to corrosion by its oxidizing power, furthermore the passive layer of oxides present on the metal surface is likely to protect the metal from being oxidized by O_3 [74].

Several artists' pigments were found to fade when exposed to atmospheric ozone even in the absence of light [113] [114] [115] [116] [117]. In particular various studies demonstrated a very high sensitivity to ozone presence of

alizarin-based pigments and dyes [113] [115] [116] [117]. Drisko et al. (1985) [113] and Shaver and Cass (1983) [117] examined some organic artists' watercolors to assess the scope of fading by ozone and thus observed that the red pigments which contain an alizarin lake are particularly sensitive to ozone damage, compared to other pigments such as organic yellows [117], triphenylmethane/copper phthalocyanine-based mauve [117] [113], quinacridone reds [113], BON arylamide reds [113], Indigo [117], Payne's gray [117], arylamide yellows [113] and chlorinated copper phthalocyanine green [113]. It has been determined that, for the most part, ozone attacks organic molecules at carbon-carbon double bonds, both in olefinic (straight carbon chain) and, more slowly, in aromatic (benzene ring) structures [114] [115]. This reaction oxidizes the organic molecule, ultimately cleaving the carbon atom framework at the site of initial ozone attack. Since these double bonds often form part of the chromophore in organic colorants, their destruction from ozone reaction usually leads to a loss of color [114][115].

The ozone fading of a colorant system was assessed to be actually a very complicated process governed by a variety of factors. Various studies, in fact, suggested that the rate of fading in the presence of ozone depends not only on the chemical nature of the colorant (particularly on the number and types of chemical bonds and atomic sites vulnerable to ozone attack), but also on the substrate into which the dye was absorbed or the pigment applied, the relative humidity and the kind of binder possibly mixed with the coloring agent that may absorb ozone, increasing contact, or protect the pigment particles [114][115][117]. Scientific proof of the significant role of the substrate in the ozone fading of colorants was given by Grosjean et al. (1987) [115] who used various materials as substrates (silica gel, cellulose and Teflon) for the deposition of the colorants alizarin, Alizarin Crimson (a

calcium-aluminum lake pigment) and their simple structural homologue anthraquinone. Grosjean et al. (1987) observed that Alizarin Crimson reacted with ozone on all substrates, yielding phthalic acid (major), benzoic acid (minor), and other minor and unidentified products. Anthraquinone did not react with ozone irrespective of conditions. Alizarin did not react on Teflon or cellulose but reacted on silica gel to yield phthalic acid (major) and other products. Because of the results obtained with Alizarin, Grosjean et al. (1987) suggested that a chemical mechanism responsible for the fading of alizarin-related colorants by ozone is consistent with the products distribution, the observed reactivity sequence, and the observed substrate-specific effects.

Grosjean et al. (1988) [116] also studied ozone fading of indigo and indigo derivatives colorants namely dibromoindigo, and colorants containing thioindigo and tetrachlorothioindigo. Under the conditions employed, indigo and dibromoindigo were entirely consumed, and the major reaction products were isatin and isatoic anhydride from indigo and bromoisatin and bromoisatoic anhydride from dibromoindigo. Thiondigo, instead, resulted significantly less reactive toward ozone than the other two samples. The results obtained induced Grosjean et al. to rationalize them in terms of a mechanism involving electrophilic addition of ozone onto the unsaturated carbon-carbon bond. According to their hypothesis, this mechanism adequately describes the observed loss of chromophore (fading) for all indigos studied and presumably applies to other indigo compounds as well. The same reaction mechanism was suggested to happen by the same authors, also during the fading by ozone of the organic colorant curcumin [118]. Furthermore, results obtained for one structural homologue of curcumin, ferulic acid, resulted also consistent with the

proposed mechanism supporting its general applicability to other compounds, including colorants, of similar structures [118].

Since ozone easily attacks carbon double bonds, one of the most vulnerable materials in its presence is rubber. Typically, cracking can be observed on the rubber surface when it is stretched and exposed to ozone. The cracks formed contribute to diminish the appearance of rubber products [119] [120][121].

1.4 Preventive Conservation

The ICOM-CC (International Council of Museums - Committee for Conservation) adopted the term Preventive Conservation (PC) in order to define "all measures and actions aimed at avoiding and minimizing future deterioration or loss. They are carried out within the context or on the surroundings of an item, but more often a group of items, whatever their age and condition. These measures and actions are indirect, that is they do not interfere with the materials and structures of the items. They do not modify their appearance". Therefore, PC aims to minimize aging and degradation by optimizing display and storage solutions. In the long term, preventive conservation is more cost efficient than remedial conservation, which can be incredibly more expensive than appropriate PC measures. Granting the optimal environmental conditions around the art objects help to minimize the pollutant amount in the microclimate within the storage items and the emissions of the packaging materials (wood, paperboard, glue, etc.) thus eliminating the need for periodical interventions. In light of the above, according to PC, the conceivable actions against museums

indoor pollution are the monitoring of the air quality and the mitigation of pollutants concentration, where necessary.

1.4.1 Pollutants monitoring

There are two general approaches to air quality monitoring: active and passive. In the active monitoring systems, the air to be monitored is pulled into the device by a pump, so a power supply is needed. In the passive sampling devices, instead, the air naturally diffuses into the trap and the contact with the pollutants is not assisted by any device. These second approach is the one that better adapts to the air quality control in museum environments, considering the spaces and their features. Furthermore, passive monitoring is generally less expensive and easier to use than active monitoring that typically requires costly, sophisticated instrumentation and technical expertise.

Cultural heritage objects require *ad hoc* environmental conditions to be properly stored or exhibited, that are generally different from an environment appropriate for human safety [1]. Furthermore, the concentration values of the pollutants of concern to art objects are of the order of ppb or ppt and the cheap and easy to use sensors available on the market can hardly detect values of 0.1 ppm [122][123][124][125][126][127][128]. Some portable devices commercially available, allow to measure pollutants in ppb but only detect the whole of corrosive gases, thus making the discrimination of a single class of pollutants impossible and, consequently, making it difficult to carry out a correct and targeted preventive action [129] [130] [131] [132]. The needed accuracy and sensitivity for the detection of specific pollutants in the order of ppb require, in fact, an indirect reading method which usually includes, at first, a sample collection and, then, an expensive laboratory analysis [133]

[1]. Developing a device able to detect and discriminate specific pollutants in the order of ppb, so that even unskilled personnel can be able to do measurements with a prompt time response, could be a major breakthrough for PC in museums, not only because of the possibility of a correct monitoring, but also of a money-saving action.

1.4.2 Pollutants mitigation

Adsorption technology has been used to VOCs abatement for years and various effective materials are nowadays commercially available. The mitigation of VOCs concentration can be reached through destruction methods or recovery methods. The destruction methods require a large consume of energy for the conversion of VOCs in other species and can often lead to the formation of toxic byproducts [134]. Recovery methods, instead, use adsorption materials capable of chemically and physically interacting with VOCs without any energy consumption [134]. Among the more efficient VOCs removers that works by physical and/or chemical interaction with the pollutants are included activated carbon, graphene, zeolites, clays, silica gel, hypercrosslinked polymeric resins and metal organic frameworks (MOFs) [134-135]. These adsorption systems are widely used owing to their low energy consumption and flexible operation [135-136]. Despite their attractive properties, every aforementioned absorber has some drawbacks. Carbonaceous adsorbents work by physical processes, to trigger also chemical processes and avoid any desorption of the physisorbed compounds due to environment variations, activation or modification treatments are requested [134-137]. Zeolites exhibit very good performance if combined with catalytically active metals but their synthesis process is complex and time-consuming and, since the pore structure is mainly mesoporous, they are unsuitable for adsorption of macromolecules. Furthermore, a high dosage of zeolite particles can lead to particles

interactions that results in their agglomeration with consequent decrease of the available surface area and thus of the adsorption capacity [138-139]. The synthesis of graphene is complicated and its severe aggregation restricts a wide commercial application as gas adsorbents [140]. As regards clay minerals, these materials provide a low-cost class of VOCs adsorbents, but their adsorption capacity at low concentration is about 10% of that of activated carbon and they thus need to be treated in order to enhance their performances [141]. Silica gel contains silicon molecules like zeolites but it has a great affinity with water that implies a poor adsorption performance under humid environment, furthermore the microporous volume is lower than the other cited systems [142]. Hypercrosslinked polymeric resins showed good performances in VOCs mitigation but they are petroleum-based materials that cannot be considered eco-friendly [143]. Metal organic frameworks have proved excellent performances in adsorptive removal of VOCs but the majority of the developed MOFs are in the form of polydisperse microcrystalline powders and are expensive [144-145].

2 Scope

The conservation of cultural heritage objects inside the museums is affected by the presence of aggressive pollutants. Granting the optimal environmental conditions around the art objects, minimizing the pollutants amount in the environment they are exposed or stored, is a very important issue to deal with for a correct conservation of works of art and historical objects in museums and archives.

The chance for a cheap and easy monitoring and concentration lowering of dangerous pollutants is fundamental for minimizing aging and

degradation. It is worth noting that only a very small percentage of all museum objects are on display; the vast majority of the items are in storage, especially in small and medium sized museums, often in unsuitable climate conditions.

Unfortunately, as already stated, the long-term protection of museum collections is currently a highly demanding goal. Both the pollution monitoring tools and the passive sampling devices on the market, suitable as concerns dimensions and costs for PC, are designed for human safety application and are thus tailored for pollutants that are not considered, except for a few of them, dangerous for art objects.

The goal of the AMAART Project, performed at CNR-ISMN in the framework of the H2020 APACHE project, was to carry out complementary research activities to contribute to the development of materials and approaches for an effective Preventive Conservation (PC) during storage and exhibition of art objects. In particular, to inhibit and slow down the ageing and degradation of artefacts in exhibition or storage environments, innovative materials with a high surface area and an appropriate surface chemistry able to adsorb selected classes of pollutants were developed taking into account mandatory features such as sustainability, biocompatibility, low-cost, efficacy and ease of use.

As regards the monitoring of some of the most dangerous pollutants for the art objects, within the AMAART projects, a contribution to the development of sensors produced for the detection of selected pollutants was carried out through advanced chemical-physical characterization of the devices during their setup and after the application tests by the CNR-ISM.

3 Methods

3.1 Aerogels development

Chitosan was used for the production of adsorbent aerogels due to its many positive features among which low cost, abundance, biocompatibility, excellent adsorption properties and antifungal properties [146][147][148][149][150][151][152][153][154]. Chitosan is a polysaccharide composed of glucosamine and N-acetyl glucosamine, derived from the deacetylation of chitin, the main component of crustaceans' exoskeleton that generally comes from food waste (Figure 1).

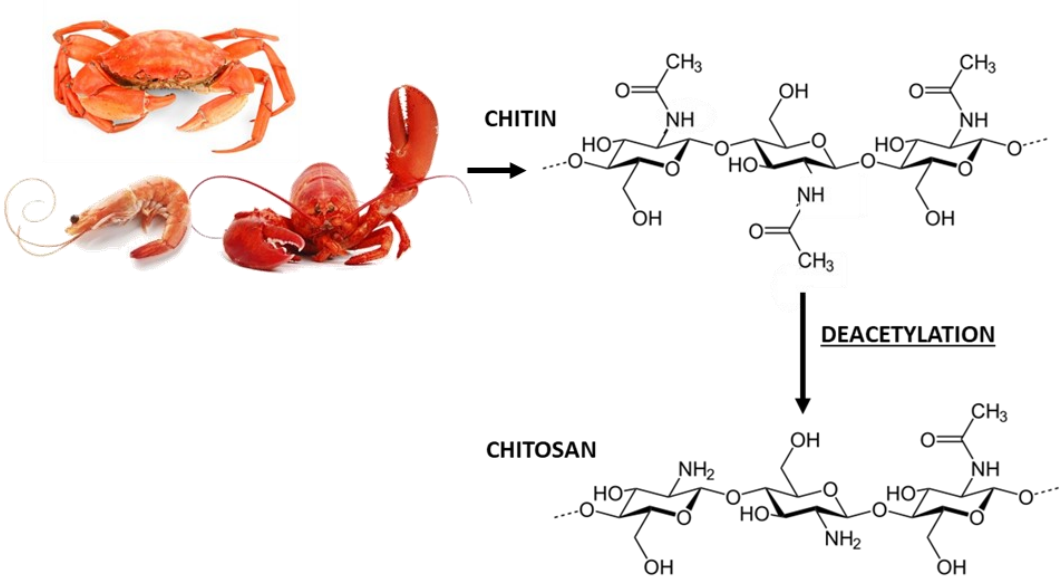

Figure 1. Pictures of some of the crustaceans from whose exoskeleton the chitosan is derived by deacetylation (left). Chemical structure of chitin and chitosan (right).

In the design of the aerogels, three crucial features were considered: pore structure, chemical functional groups and easy production. The pore structure is fundamental to grant a specific surface area, functional groups have the important role to allow the pollutants chemisorption and an easy production is needed for a wide application.

The adsorption efficiency of chitosan towards the selected gas pollutants comes from the ability to chemically bond aldehydes.

Furthermore, it is possible to obtain high porous structure from chitosan to enhance the contact between the adsorbed and the pollutant [155]. In addition to the chemical composition of the material considered, a large specific surface area is indeed critical for reactive gas adsorption. Since both the chemical properties and pore structure of an adsorbent determine its adsorption capacity, chitosan-based aerogels with a porous structure were produced.

3.1.1 Starting solution

The first step for the production of the aerogels is the dissolution of the chitosan to obtain a chitosan solution.

For chitosan dissolution, several acid solutions were prepared varying both the chitosan concentration and the acid to dissolve it, with the aim of find the optimal blend for the production of chitosan-based aerogels with a porous structure and efficient adsorption properties towards some VOCs. Indeed, the chitosan aerogels properties can be modified by changing the solvent as well as the acid solutions concentration used for chitosan solubilisation.

In the literature, some studies were conducted on the chitosan dissolution using different carboxylic acid also for the fabrication of membranes [156-157] In this research, A.A., AD.A., O.A. and S.A. were used to dissolve chitosan (figure 2). A.A. is one of the most popular carboxylic acids used for the dissolution of chitosan and, since it is a monocarboxylic acid, it serves only as a proton donor to protonate the chitosan amines that thus become positively charged and makes chitosan a water-soluble cationic poly-

electrolyte [158]. According to the literature [158-159], di- and tricarboxylic acids can be used as dissolution agents as well as cross-linking agents: multicarboxylic acids can both provide protons for chitosan dissolution and create an interaction with the polymer through the functional groups of the acids, changing the features of the chitosan solutions [157].
In table 1 the abbreviations used to describe the different chitosan solutions, from which derived the aerogels, are shown.

Table 1. Abbreviations of the various samples

	Composition	
Abbreviation	carboxylic acid	Chitosan
Chit A.A. 2L	A.A. high conc.	low conc.
Chit AD.A. 2L	AD.A. high conc.	low conc.
Chit O.A. 2L	O.A. high conc.	low conc.
Chit O.A. 2H	O.A. high conc.	high conc.
Chit S.A. 2L	S.A. high conc.	high conc.
Chit S.A. 1H	S.A. low conc.	high conc.

The chitosan used in this research was of medium molecular weight and purchased by Sigma Aldrich.

The listed carboxylic acids solutions were prepared and the chitosan was added in given percentages by weight. After the addition of the chitosan, the solution was stirred until a complete dissolution of the polymer was reached. The resulting chitosan solutions showed different viscosity according to the acid used as dissolvent agent, its concentration and the amount of added chitosan.

3.1.2 Freeze-drying

To develop high porous chitosan-based systems, a freeze-drying process was used. Freeze-drying can be successfully used to fabricate aerogels in a

cost-effective way. Most of the studies concerning the production of polymer aerogels used the supercritical drying technique. This kind of process is highly effective but also quite costly [160]. Compared to freeze drying, supercritical drying is a more complex technique, requires expensive raw material and a lot of energy consumption and CO_2.

Freeze-drying consists in froze the sample and place it under vacuum in order to remove water or other solvents. In this way, the ice can change directly from solid to vapour phase without passing through the liquid phase (sublimation). The sublimation allows to obtain extremely porous systems, i.e. aerogels. Aerogels are a unique class of materials with special features such as high surface area, high porosity, highly cross-linked structure and low density.

3.1.3 Aerogels functionalisation

The chitosan-based aerogels were functionalised using different kind of fillers to enhance both their antimicrobial activity and their adsorption efficiency with respect to the classes of pollutants selected for this research.

3.1.3.1 Functionalisation with Ag

Chitosan is a natural polymer that has many useful features among which antimicrobial properties. However, when left exposed for a long period of time, it is necessary to improve both its antimicrobial and antifungal activities.

To that end, the chitosan was combined with silver (Ag) nanoparticles (NPs) whose bactericidal effects have been observed since ancient times [161-162-

163]. The antibacterial efficacy of Ag NPs is related to various parameters including particle size, shape and concentration [164-165-166].

The results of different studies [167-168] showed that smaller Ag NPs have a higher antibacterial activity as they better attach to the surfaces of cell membranes than do larger AgNPs. AgNPs were, therefore, prepared to be used as filler. The AgNPs were obtained by using a facile in situ photoreduction method.

3.1.3.2 Functionalisation with alkaline particles

Alkaline particles were chosen as filler to improve the adsorption efficacy of the aerogels towards organic acids.

The functionalisation was carried out adding to a chitosan solution the C.C. particles.

The added C.C. particles were homogeneously dispersed in the chitosan solution (figure 8).

3.1.3.3 Functionalization with A.NPs

The analysis conducted in previous studies provided evidences for an efficient reactive uptake process of some organic acids such as A.A. and formic acid on A. particles [171-172]. A dispersion of A. was then chosen, in addition to alkaline particles, to improve the aerogels adsorption efficacy towards organic acids.

The aerogels functionalized with A. were prepared from a commercial dispersion (Alpha Aesar). In this case, the chitosan dissolving agent was added to a dispersion of A. NPs in H_2O and then the chitosan was also added.

3.2 Sensors development

Within the H2020 APACHE Project, the CNR-ISM (Consiglio Nazionale delle Ricerche – Istituto di Struttura della Materia) research group developed novel physical sensors characterized by high sensitivity thanks to the nanostructuring of active materials, mechanical flexibility and low production cost. The sensors were developed by application of active materials on flexible plastic substrates.

In particular, the first step of the activity focused on the developing of the basic sensors that were later integrated as part of a smart active multi-sensor for the early detection of degrading species. In order to achieve a high sensitivity, materials with a different reactivity toward selected VOCs have been developed and the sensitivity of each one has been enhanced through the surface nano-structuring. The polyimide material Kapton (registered trademark of DuPont) was chosen as substrate for the sensors production due to its features i.e. flexibility, low cost per unit area, chemical inertness, low electrical conductivity and stability in temperature (up to 400 °C in case of absorbing sensing materials).

Every active material was structured into a sensor by CNR-ISM and was tested by CNR-ISM in collaboration with CNR-ISMN (figure 10).

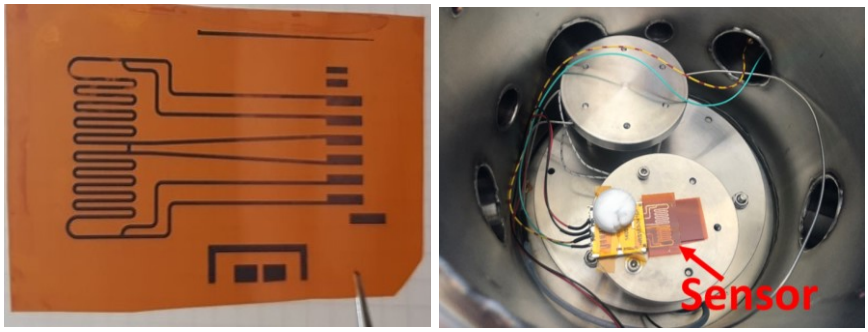

Figure 10. Picture of one of the sensors produced by CNR-ISM (left), picture of the sensors inside the testing chamber.

Sensors with three sensing materials were produced: copper, silver and zinc. These three metals were chosen according to their sensitivity towards the VOCs to be monitored, that were selected for this research. In particular copper was selected because of its high sensitivity towards A.A., formic acid and formaldehyde. Silver was chosen, instead, as reference material due to its low reactivity to the cited VOCs, with a view to the further development of a VOC's multisensor.

The sensing performance of the sensors were evaluated in a specifically developed testing chamber. IONVAC PROCESS SRL designed the setup of a vacuum chamber for the test campaigns. The sensors' sensitivity was first calibrated as a function of the pollutants' concentration by inserting a given concentration of the selected VOCs in the chamber. The liquid pollutants were injected by a syringe within the test chamber and diluted by dry compressed air (figure 11 and 12).

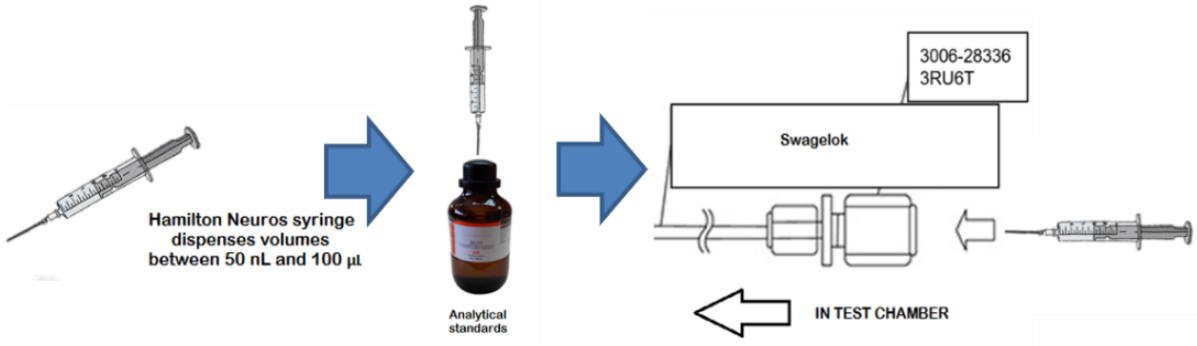

Figure 11. Drawing illustration resuming the procedure for injecting the liquid pollutants within the testing chamber.

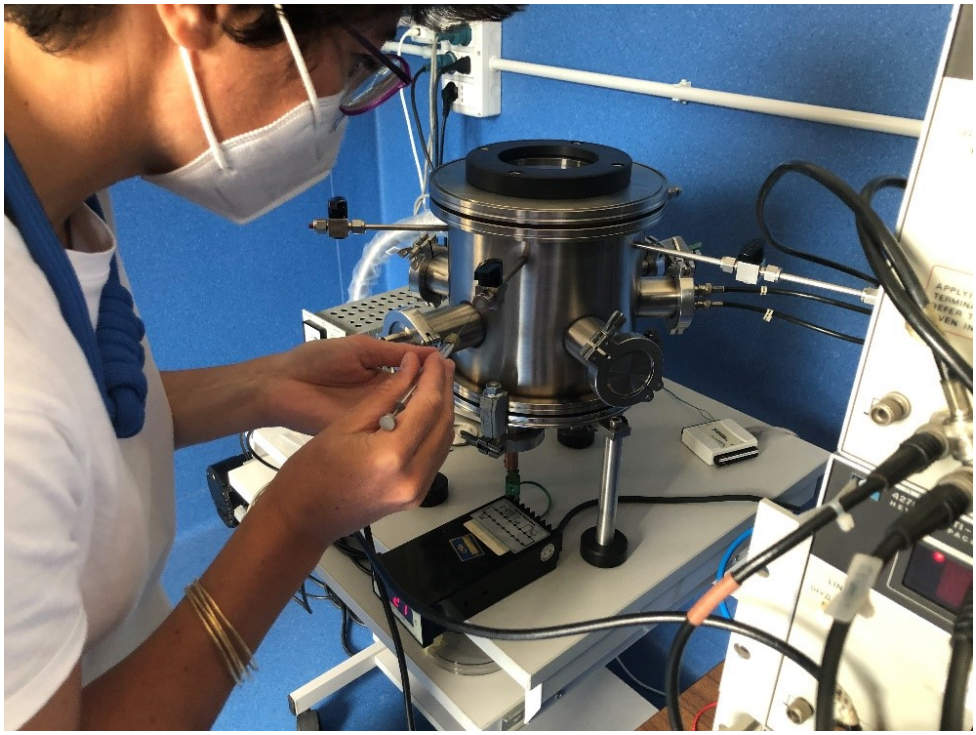

Figure 12. Picture of the insertion of the pollutant in the chamber.

The pollutants were injected under high vacuum conditions to allow their vaporization. Continuous dry air injection diluted the concentration down to the desired concentration values.

The sensors' signals were measured by impedance meters so as to make it possible to apply impedance spectroscopy techniques, whose output parameters depend on the higher sensitivity of the changes in the electrical properties of the active material compared with the mere resistance value.

3.3 ATR-FTIR Spectroscopy

Attenuated Total Reflectance Fourier Transform Infrared (ATR-FTIR) spectroscopy was used to analyse the chitosan-based aerogels as such and

after their exposure to the selected pollutants as well as the corrosion products of some metal coupons exposed in polluted environments. The spectra were collected using a Nicolet iS50 spectrometer (Thermo Fisher) equipped with an ATR accessory. The measurements were recorded using a diamond crystal cell ATR using 32 scans at a resolution of 4 cm^{-1} and no ATR correction was applied to the data.

Infrared spectroscopy provides information related to the presence or absence of specific functional groups. In the infrared spectroscopy technique, the molecules absorb frequencies (infrared radiation) that are characteristic of their structure. These absorptions occur at resonant frequencies, i.e. the frequency of the absorbed radiation matches the vibrational frequency. The energies are affected by the shape of the molecular potential energy surfaces, the masses of the atoms, and the associated vibronic coupling. Changes in relative band intensities and shifts in the frequency of absorption bands indicate changes in the chemical structure or changes in the environment around the sample. FTIR-ATR was thus used to determine resultant chemistry following chemical modifications. The ATR accessory operates quantifying the changes that happen to an internally-reflected infrared beam, once it comes into contact with the sample. To do this, an infrared beam is focused onto a crystal with a high refractive index at a set angle: the infrared light travels through the crystal, it is totally internally reflected at least once at the crystal-sample interface and finally the reflected light travels to the FTIR detector (figure 13). During the internal reflection, a part of the IR light travels into the sample, where it can be absorbed. This is called the evanescent wave. The penetration depth of the evanescent wave into the sample is defined by the refractive index difference between the sample and the ATR crystal.

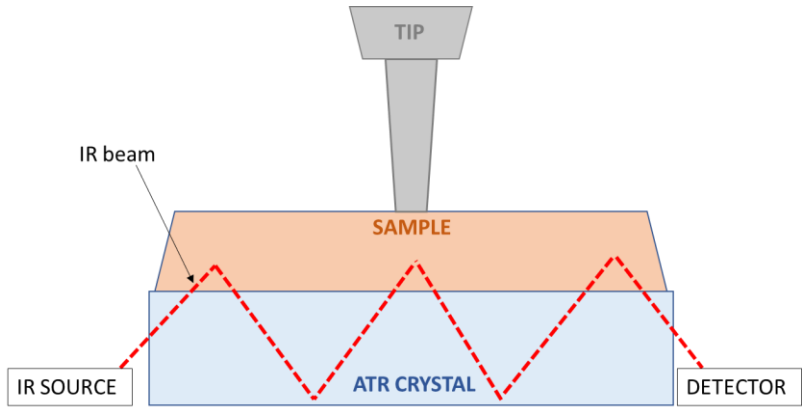

Figure 13. Schematic illustration representing the operation of the ATR accessory.

This initial wave only protrudes by a couple of microns (between 0.5 μ and 5 μ) beyond the surface of the crystal, and into the sample itself. Therefore, the sample has to be in good contact with the surface of the crystal. To grant an optimal contact between sample and crystal, the sample is pressed down by a swivel tip (figure 13 and 14). The detector records the attenuated IR beam as an interferogram signal, which can then be used to generate an IR spectrum. This technique allows recollecting the samples since no sample preparation is required. The term "Fourier-transform infrared spectroscopy" is based upon the Fourier transform process, which is required to convert the raw data into spectra.

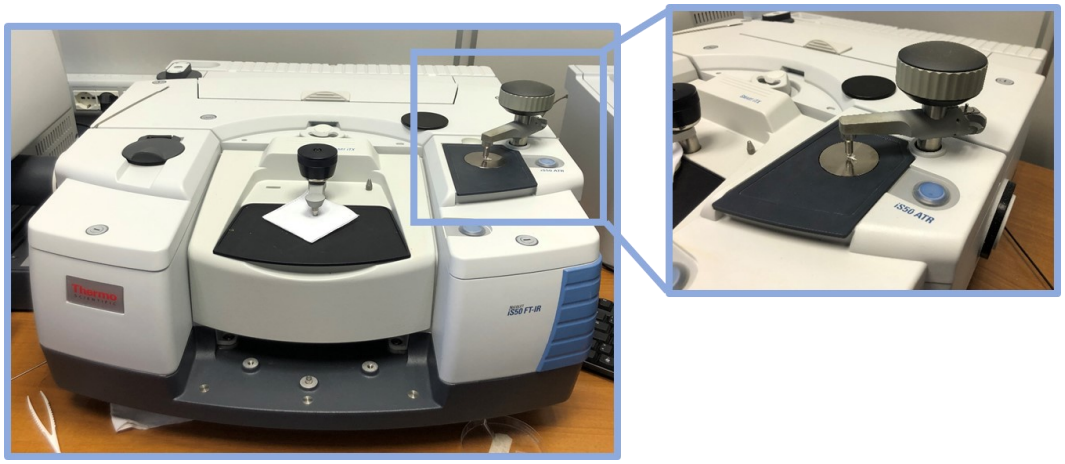

Figure 14. Picture of the Nicolet iS50 spectrometer equipped with an ATR accessory used for the infrared spectroscopy analysis. On the right, a magnification of the portion of the instrument with the swivel tip and the crystal are shown.

3.4 SEM

Depending on the carboxylic acids as solvent and crosslinker used, the chitosan solution properties can change. Therefore, a characterization of the different chitosan-based aerogels obtained using the previously listed carboxylic acids was conducted by scanning electron microscopy (SEM).
Micro-chemical and morphological characterisations were performed by means of a high brilliance LEO 1530 field emission scanning electron microscope (FE-SEM) apparatus equipped with an energy dispersive X-ray spectrometer (EDS) INCA 450, respectively, and a four sector back-scattered electron (BSE) and secondary electron (SEI) detectors (figure 10). SEM allows resolving objects ranging from part of nano-metre to micro-metre compared to light microscope that has a magnification in the range of 1000 and resolution of 200 nm. Interacting with the sample, the electron beam reveals useful information about it including its surface features, size and shape of the features, composition and crystalline structure. The interaction of the electron beam with the specimen can occur in different ways. The incident electrons can give enough energy to the specimen electrons, mainly in the K shell, to change their path and induce an ionization of the specimen atoms. The ionized electrons escaping the specimen atoms are called secondary electrons. These electrons then move to the surface of the specimen and undergo to elastics and inelastic collision until reaching the surface. Secondary electrons are characterized by a low energy (~ 5eV), consequently only those electrons that are close to the

surface (~ 10 nm) can escape the surface to be detected for imaging the topography of the specimen. When the incident electrons hit an atom directly, they can be reflected or back-scattered. Different atomic type of atoms results in a different rate of backscattered electrons and hence the contrast of the image varies as the atomic number of the specimen change, usually atoms with higher atomic number will appear brighter than those that have lower atomic number. The incident electrons can also pass through the sample without any interaction with their atoms (transmitted electrons) and without losing any energy, being then scattered in an elastic way. If the bombarded atoms of the specimens release electrons in an excited state, in order for the atom to return to the ground state, an excess of energy is released producing Auger electrons, X-Rays and cathodoluminescence. The X-Rays emission produce an energy signature that is a unique characteristic of each element. The X-Rays are thus used to identify the elements and their concentrations in the specimen. This technique is called energy dispersive spectroscopy (EDS) since the energy of the X-rays is detected. EDS is mostly used for qualitative analysis of materials but is capable of providing semi-quantitative results as well. Since the electrons are easily scattered in air most of the electron microscopes operate under a high vacuum (figure 15). The electron microscopes basically consist of three basic components: electron gun, vacuum and column. The electron gun emits the electron beam (which is held within a vacuum) and follows a vertical travel path through electromagnetic fields and lenses. The electron beam is focussed by objective lens on the specimen. The beam is rastered across the surface of the materials with the help of deflector coils. The different signals produced by the electron beam hitting the samples are detected by the detectors and converted to signals.

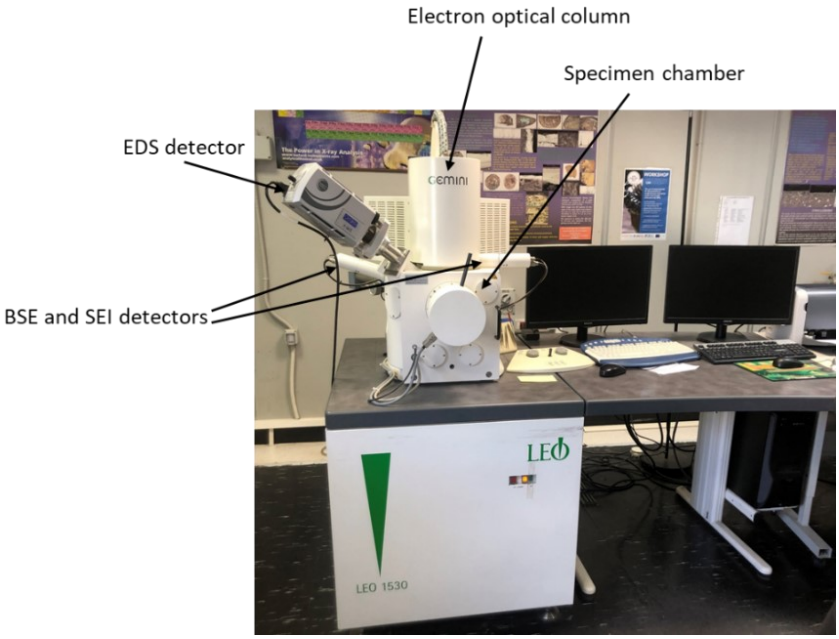

Figure 15. Picture of the FE-SEM LEO 1530 used in this research project.

3.5 AFM

Atomic force microscopy (AFM) was used to study the surface roughness of the sensors before and after their use in controlled and tailored polluted environments.

Within this research project, a Multimode 8 microscope equipped with a Nano Scope V controller (Bruker, USA) and a type E piezoelectric scanner (Veeco) was used. The images were captured operating in Peak Force Tapping mode and using ScanAsyst-Air (ScaAsyst Air probe – Bruker) tips. A scan rate of 0.8 Hz was employed at a resolution of 512 pixels/line.

AFM is a high-resolution non-optical imaging technique that allows accurate and non-destructive measurements of the topographical properties of a sample surface with very high resolution. The main part of the AFM is the cantilever/tip assembly, often referred to as the probe. The AFM systems involve scanning a sharp tip over the sample surface in a

raster pattern. The tip is integrated near the end of a flexible AFM cantilever and is usually made of silicon nitride or silicon. The vertical and lateral position of the probe on the sample surface is controlled by a piezoelectric ceramic scanner. The tip movements result in cantilever deflections that reproduce the surface roughness. A laser beam tracks the cantilever deflection and hits on a sensitive photodetector (figure 16). An electronic feedback loop is employed to control the vertical extension of the scanner and hence to keep the probe-sample force constant during scanning. The AFM tip traces a path whose coordinates generate a three-dimensional topographic image of the sample surface. The coordinates that the AFM tip tracks during the scan are combined to generate a three-dimensional topographic image of the surface.

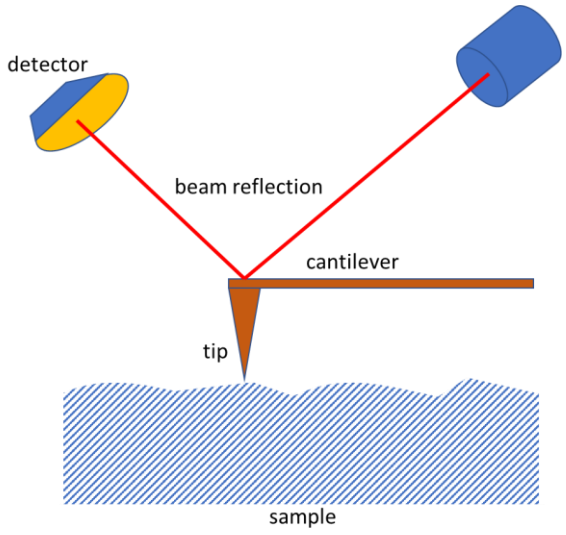

Figure 16. Schematic illustration representing the operation of the AFM.

3.6 Adsorption and chemisorption tests

The adsorption properties of the prepared aerogels were investigated by studying their interactions with some aldehydes and organic acids, that

were selected as representative pollutants. The tests were chosen in order to study both the physisorption and chemisorption efficiency vis-a-vis the selected pollutants of the developed systems. Weight gain tests were carried out to monitor the physisorption capacity of the aerogels whereas tests with metal coupons were conducted to study their mitigation efficiency. ATR-FTIR analysis helped to observe any chemical interaction of the pollutants with the chitosan and/or the fillers to confirm the chemisorption.

3.6.1 Weight gain tests

The chitosan-based materials were exposed to a certain amount of pollutant in a sealed vessel and their weight gain was monitored. In order to study the physical interaction between absorbents and volatile organic compounds, the tests were carried out using an excess of pollutants. The amount of pollutant (liquid phase) inserted in the sealed vessels was such as to obtain a saturated environment.

According to the results obtained monitoring weight variations and analysing FTIR data of the first samples prepared, a measurements process was defined to assess the adsorption efficiency of the developed systems. The aerogels were weighed after every predetermined time of exposure to the pollutant (24, 48, 72, 168 h) and after desorption treatment on a heated plate at 35°C (5, 24, 48 h).

The desorption treatment was applied in order to monitor the weight gain of the aerogels after the desorption of the physisorbed pollutant.

The results of the weighing during the aerogels exposure to the pollutants and during the desorption were presented as weight gain percentage and were calculated as follows:

Calculation during the exposure to the pollutant

$$\frac{weight\ gain\ after\ exposure - weight\ t_0}{weight\ t_0 \cdot 100}$$

Calculation during the desorption on a heated plate

$$\frac{weight\ gain\ after\ desorption - weight\ t_0}{weight\ t_0 \cdot 100}$$

The words *weight gain after exposure* and *weight gain after desorption* means the weight of the aerogel measured after a certain period of time of exposure to the pollutant and after a certain period of time on a heated plate, respectively.

To look at the weight trend of the aerogels, the weight gain percentage are shown using bar charts. The results obtained during the exposure to the pollutant were combined with those obtained during the desorption process to study the efficiency in physisorbing the pollutant at high concentration and the release during the desorption. The last bar of the bar chart where the weight gain values measured during the desorption are presented, provides an information of the retain capacity of the aerogel.

An example of bar charts made to show the weight gain percentage trend is shown hereafter in figure 19.

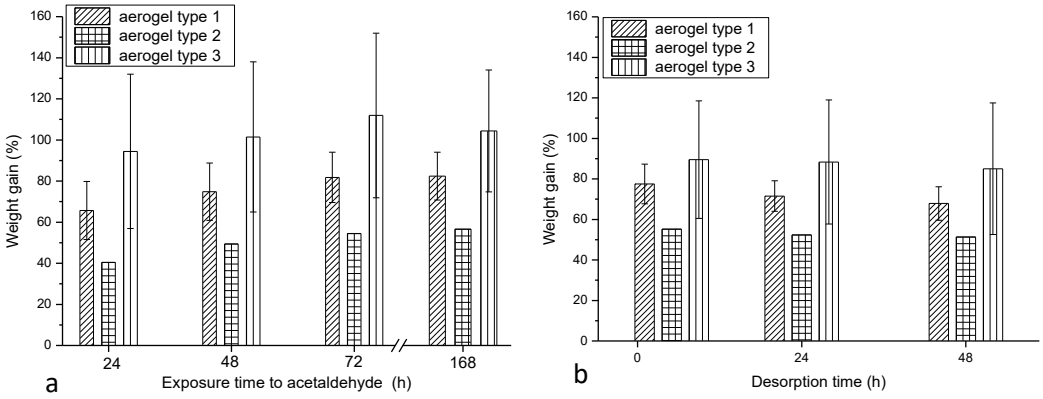

Figure 19. a) Weight gain versus exposure time to acetaldehyde and b) weight gain versus desorption time of three different type of chitosan aerogels developed during the research activity.

3.6.2 ATR-FTIR aerogels analysis

ATR-FTIR analysis were first conducted to characterize the developed aerogel and check the functional groups available for a chemical interaction with the pollutants.

ATR-FTIR analysis were subsequently carried out on the aerogels before their exposure to the selected pollutants (as such) and 48 h from the beginning of the desorption process (3.6.1 Weight gain tests). The choice of analysing the aerogels at the end of the desorption process was dictated by the need to study the chemical interaction of the pollutants with the chitosan and the fillers avoiding any overlapping related to a physical interaction.

Aldehydes can be chemically adsorbed by polymeric amines such as chitosan via a reaction that leads to the formation of a Schiff base (figure 22) [151-153]. By means of ATR-FTIR analysis the chemical interaction of the aerogels with the pollutants was verified. Possible changes in the spectra,

collected analysing the aerogel after their exposure in a polluted environment, were checked to that effect.

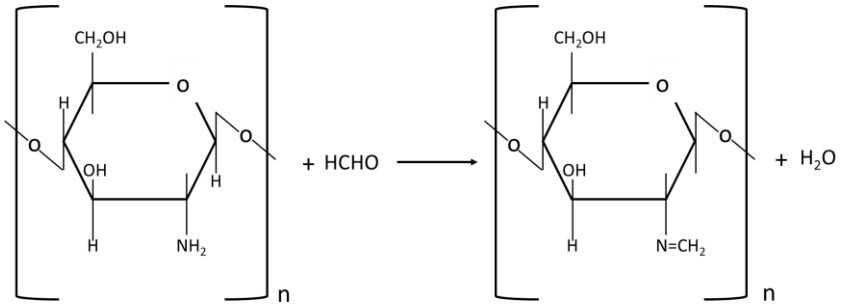

Figure 22. Reaction scheme between chitosan and formaldehyde.

The main peaks associated to the chemisorption of aldehydes were identified and the modification of their intensity was used to monitor the adsorption capacity of chitosan aerogels. Specifically, the peaks at about 1560 cm^{-1} and 1640 cm^{-1} are assigned to NH_2 scissoring vibrations of glucosamine monomers and to C=O vibration of acetamide groups, respectively. The intensity of the peak at 1640 cm^{-1} increases with respect to that of the peak at 1560 cm^{-1} after exposure to acetaldehyde. This is due to the occurrence of a chemical reaction between the aerogel surface and acetaldehyde that involves the generation of new chemical bonds between aldehyde molecules and amine groups of chitosan. The ratio between the intensity of the absorption band at about 1640 cm^{-1} and that of the band at 1560 cm^{-1} were thus considered to evaluate the presence of chemisorbed aldehyde [173] (Figure 23). 173

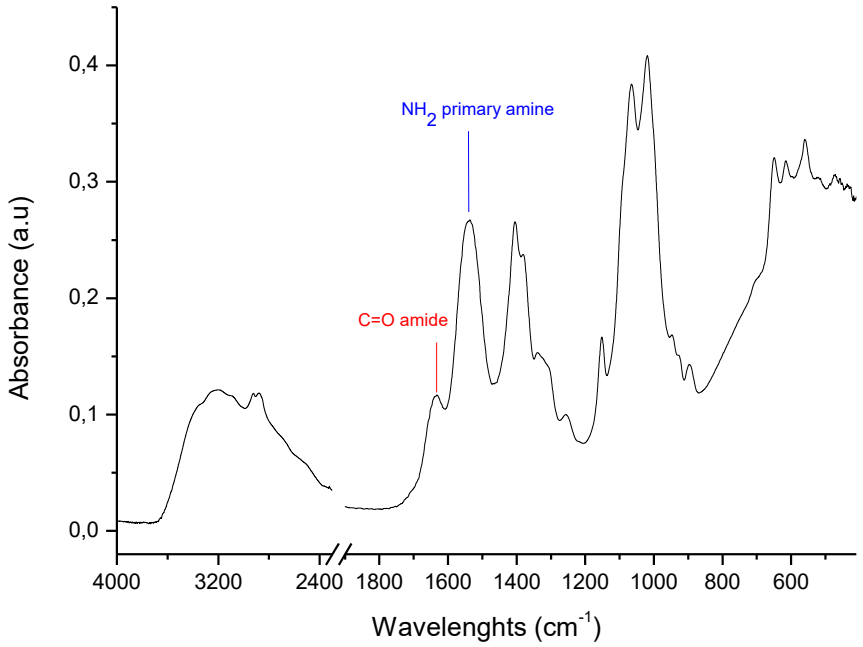

Figure 23. Infrared spectra of a chitosan aerogel as such. The band related to the acetamide and that related to primary amine are marked in the spectrum.

3.6.3 Tests with coupons

Coupons are samples of standard materials used as passive sampling devices to provide data related to the air-quality. These samples are used as "cavies" since they get damaged (corrode) quickly as compared to an art object and allow to easily and cost-effectively be aware of the corrosion power of an environment by a subjective scoring. They can also be used for an accurate study of the presence of specific dangerous pollutants, provided the corrosion products are characterized by means of techniques such as FE-SEM-EDS, FTIR and X-ray diffractometry (XRD). Coupons can be made of different materials, sometimes the same of those composing the art objects of the collection in study.

The most suitable solution for monitoring air corrosivity and the mitigation efficiency of the developed aerogels is the use of metal coupons, that grant

a fast-response and allow an easy trace back of the most dangerous indoor pollutants like VOCs, because of the role they play on metal oxidation [1][174].

Test using alloy coupons were thus carried out to check the efficacy of the developed aerogels in protecting from the degradation metalwork exposed to polluted environments. Copper alloy disks and lead disks were chosen as coupons for the tests. The copper alloy coupons were chosen because of their affinity with the bronze alloy usually used in modern bronze statues (5% Sn, 5% Zn, 5% Pb, 85% Cu) whereas lead coupons were chosen due to the high sensitivity of lead towards some of the selected VOCs [27-29-87-129].

Tailored polluted environments were created inside sealed glass vessels by inserting the same amount of pollutant. The metal coupons were exposed to the pollutants for a certain period of time with and without a chitosan-based aerogels inside the vessel.

After a determined period of time, the degree of corrosion of the coupons was checked by means of ATR-FTIR. The spectra of the coupons exposed at the same polluted environment in the presence of the adsorber and without it were compared. The intensity of the bands related to the corrosion products in the FTIR spectra collected analysing the coupons was used as an indicator for the corrosion aggressiveness of the environment inside the vessels. Accordingly, checking the intensity it was possible to state the mitigation efficacy of the aerogels in the vessels.

3.7 Tests of antifungal properties

The antifungal properties of the aerogels functionalised with silver was investigated. The aerogels were required to provide a certain degree of antifungal effect in order to guarantee a safe environment for the exhibited artworks and to inhibit the growth of common and widespread fungal strains. This property is particularly important when the aerogels are in an uncontrolled environment. Indeed, a raise of relative humidity can cause germination of fungal spores, a rapid growth of the mycelium and the colonization of the environment by fungi. Therefore, it is important to determine if the aerogels can resist to a fungal colonization and if they can also inhibit the fungal growth. The antifungal effect was tested on aerogels without any filler or additive and on functionalized ones. In particular, different amounts of silver were used in combination with the aerogels in order to enhance the fungal growth inhibition and their properties were tested.

For this study, the fungal specie Aspergillus niger was selected as model organism. *A. niger* is a filamentous ascomycete that is ubiquitous in soil and is among of the most abundant species present in warm environments. It grows aerobically on organic matter and it is a common contaminant on various substrates. It is prevalent in residential areas, even in urban settings, and is found in both indoor and outdoor environments. The fungal strain was purchased from the Mycotheca Universitatis Taurinensis (*Aspergillus niger* MUT 477). This strain was selected due to its first isolation from an indoor environment. The strain was replicated using malt extract agar as culture medium, cultivated in the dark at 25°C for optimal growth and then stored at 6°C. All the samples were sterilized on both sides for 30 minutes under UV light before inoculation. Solid inocula of the fungal strain were

transferred on Petri dishes containing malt extract agar, placed aside the aerogelsand incubated in the dark at 25°C. All tests were conducted in triplicates. Triplicates of the fungal strain alone were used as control (figure 25) and all samples were let grow until the control fungus covered the entire Petri's surface. According to the control growth, the first test lasted 16 days while the second test lasted 11 days. At regular interval, pictures of the Petri dishes were acquired, and the fungal growth evaluated by image analyses through ImageJ software. The growth inhibition effect of each aerogel was indicated by the percentage of the aerogel surface not covered by the fungus at the end of the experiment.

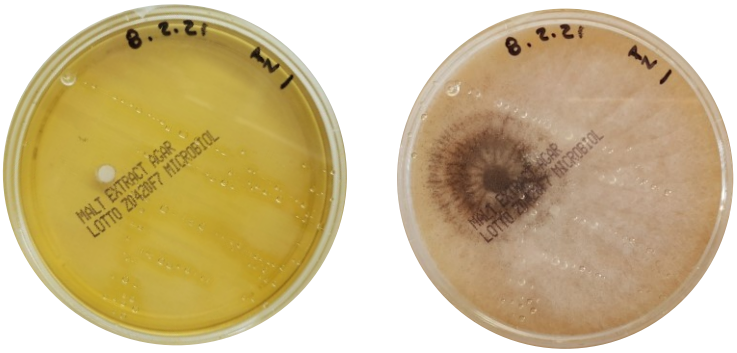

Figure 25. Pictures of a Petri dish inoculated with the fungus (control) at the beginning (left) and at the end (right) of the experiment.

4 Results

4.1 Sensors characterization

The chemical, morphological and structural properties of the sensing materials prepared within the APACHE Project were investigated both during their development and after the tests.

Investigations were carried out as well to detect any possible morphological and chemical modifications of the sensing materials following their exposure to tailored atmospheres.

The characterization of these materials was performed by using complementary techniques aimed at detecting the presence of surface nanostructures and to evaluate the quality and homogeneity of the deposited film and to detect as well any alterations of the sensors 'metal tracks after being exposed to the selected pollutants.

A first visual investigation on the sensors was conducted. The different behavior of the metal tracks 'surface depending on to the pollutants they were exposed to appeared evident through a visual observation of the samples.

Optical microscopy images were then captured to observe the metal tracks in more detail. The copper sensor AP059 Cu was exposed to a very high concentration of pollutant compared to AP054 Cu and AP058 Cu in order to study the behavior of the sensor at his final stage of operation. As a consequence, the images acquired and the corrosion products detected on this sensor could be considered as a sign of the end-of-life of the sensor. Optical microscopy images were captured to observe any visually perceptible degradations of the metal tracks.

During the tests conducted by the ISM research group on the performances of the sensors in polluted environments, the feedback of the zinc sensor's impedance exposed to acetic acid showed an opposite behavior with respect to that of copper sensors. This result suggested a different interaction mechanism of the zinc with respect to copper towards acetic acid. As for the copper sensors, one of the zinc sensors used for the tests with acetic acid was exposed to a very high concentration of acetic acid with the aim to study its behavior at its final stage of operation and to detect the formation of corrosion products.

The comparison images of the zinc sensor's track with that of the copper sensor after exposure to acetic acid showed a corrosion of the metal quite different in terms of morphological surface modifications. This confirms that a different interaction between the pollutant and the metal occurs at the zinc surface, in agreement with the results of the tests.

The sensing materials were characterized FE-SEM and AFM to evaluate the morphological properties at micro- and nanoscale level.

The FE-SEM images of the sensing materials exposed to tailored polluted environments for the calibration tests showed a modification of the surface morphology compared to the sensing material as such, as a consequence of the development of corrosion products.

Furthermore, comparing the FE-SEM images of the sensing materials after their exposure, surface differences can be noticed, probably due to a different behavior of the sensing materials depending on the pollutants they were expose to.

As regards the sensing materials exposed to acetic acid, formaldehyde and acetaldehyde, the FE-SEM images showed the presence of corrosion products spherical in shape and of a comparable diameter of about 100 nm.

The possible modifications undergone by the sensing materials surface after the exposure to pollutants were also evaluated by AFM measurements. The 3D images in figure acquired by means of AFM, shows a difference in the distribution of the surface nanostructures of the as such sensing film from those of the sensing materials exposed to formic acid and acetaldehyde.
Micro-ATR analysis were carried out on the sensors 'tracks after their exposure to the selected pollutants to examine the corrosion products developed by the presence of the VOCs.

A deeper study was then devoted to the copper sensors' sensitivity in tailored polluted environments varying parameters such as relative humidity and time of exposure. Further analyses on the possible related modifications of the metal tracks were conducted.
A preliminary study of the responsiveness of the sensors vis-à-vis the different parameters set was conducted on the copper sensors. The sensors' tracks were characterized after exposure to acetic acid in different environmental conditions by means of FE-SEM, optical microscopy and ATR-FTIR.

The SEM images show the presence of corrosion products in all the three selected samples. The sensors exposed to the same concentration of acetic acid (AP054 Cu and AP058 Cu) exhibited the presence of similar corrosion products whereas the surface of the tracks exposed to a higher concentration of acetic acid showed a significantly more degraded surface.
Furthermore, attenuated total reflectance infrared spectroscopy (ATR) analysis were carried out on the sensing materials, to perform a qualitative analysis of the possible products resulting from the interaction between the pollutant and the metal tracks. In the ATR-FTIR spectra collected, the presence of bands related to the presence of corrosion products is observed.

Once concluded the preliminary tests on the single sensors, ISM produced the multisensors using a different mask for the sensing materials deposition on the Kapton substrate to host more than one material while maximizing the exposed area (figure 35).

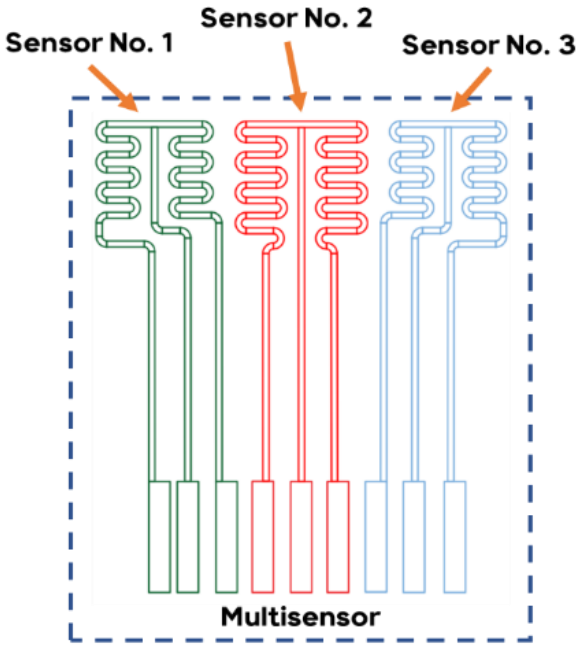

Figure 35. Sketch of the multisensor.

Analysis on each sensor of the multisensors produced by ISM were also carried out by means of optical microscopy, micro-ATR, FE-SEM and AFM. For each sensor, the spectrum recorded on a reference metal strip (covered by kapton and not exposed to the pollutants) was compared with the spectrum recorded on a working metal strip (directly exposed to the pollutant).

The results confirm that the copper sensors are sensitive to the presence of acetic acid and that the sensors signals measured by impedance meters are connected to that kind of degradation of the metal tracks.
A different comparison was made for the zinc metal tracks of the same multisensor, since the extensive degradation of the metal led to a depletion of the metal track whose signal resulted covered by the one of the kapton substrate. In the literature, the reaction of the zinc exposed to acetic acid is described as a circularly shaped reaction since it displays radially grown corrosion products that form ringlike disks [175-176].
The surface modifications of the zinc metal strip due to the exposure to the pollutants are clearly observed by optical microscopy.

Similar studies were also carried out on the silver metal strips. After the exposure to acetic acid, the silver sensors, despite the lower sensitivity of this metal towards VOCs compared to copper and zinc, showed the presence of strong adsorption bands on their surface, specific of acetate salts and carbonate species [177-178].

SEM analysis were also conducted to study the morphology of the sensors metal tracks after their exposure to the pollutants. FE-SEM images of the exposed part of the metal tracks compared to that of the covered ones, showed a significant difference of the surface morphology; all the three sensors analysed show that those exposed to the pollutant have a larger amount of corrosion products confirming the advanced corrosion process activated during the exposure. Furthermore, the images of the working part of the zinc sensor confirmed the presence of radially grown corrosion products, typically induced by acetic acid. Among all the three sensors, the silver ones appeared to be the less damaged; silver is indeed the metal that is less susceptible to organic acids attack.

To study more in dept the morphology of the track sensors, AFM analysis were also conducted on their surface.

The AFM analysis carried out on the sensors confirmed what observed by FE-SEM microscopy. The surface of the exposed part of the sensors appears more irregular than that of the reference part due to the development of corrosion products by the pollutant interaction. As regards the zinc strips, the result obtained on the exposed one apparently show a smoother surface. This result is due to the excessive fluctuation of the pitches on the surface that cannot be properly revealed by the instrument tip.

4.2 Aerogels characterizations

4.2.1 SEM - Morphology

The porosity of the aerogels structure is an important parameter to be considered since most adsorption involves the co-existence of physisorption and chemisorption. A high porosity, in fact, grants a major interaction of the chitosan matrix with the gas pollutants and thus better performances in the mitigation.

The freeze-drying technique was used to produce the aerogels in order to obtain a chitosan matrix structure as porous as possible. For the development of new chitosan-based aerogels various dissolving agents that would allow the formation of porous and strong structured aerogels were used. The first characterization of the chitosan-based aerogels was thus focused on checking the porosity of the structure of the developed systems. FESEM analysis were carried out to study the pores size and their interconnection.

The dicarboxylic acids act as solvents and, at the same time, improve the properties of the chitosan aerogels due to the ionic cross-linking and hydrogen bond formation [157]. Different concentrations were used in order to find the best formulation that allowed for a good porosity of the final aerogels and a high chitosan concentration.

Since the more the free amino groups of the chitosan chain are available the more they can react with pollutants, tests were made to determine the lower concentration of O.A. and S.A. needed to completely dissolve chitosan. Once completed these tests, aerogels Chit O.A. 2H and Chit S.A. 1H were produced, analysed by means of FE-SEM and chosen as best formulations.

As previously described, to enhance the adsorption properties of chitosan, composite materials were prepared by combining alkaline nanoparticles (C.C.), AgNPs and A.NPs with chitosan aerogels.

FE-SEM analysis showed that a good porosity was obtained for all the aerogels produced except for the one obtained from a solution of AD.A. and chitosan.

Yet after careful consideration, the most uniform and solid structure with a high porosity and a considerable connection between the pores channels results that of the aerogels obtained from a S.A. solution added with chitosan.

4.2.2 ATR-FTIR Chemical characterization

The chemical characterization of the developed materials was carried out by means of ATR-FTIR to check their final composition after their production. The bands in the ATR spectra acquired analysing the aerogels were compared to those collected analysing the starting materials they were composed of.

4.2.3 Antifungal properties

Fungal growth inhibition properties of aerogels obtained from an A.A. solution added with chitosan and functionalized with different percentage of Ag NPs were assessed measuring the percentage of aerogels surface not colonized by the fungus.

Aerogels containing only chitosan were not very effective against the fungal growth and were almost completely colonized by the fungus. This is probably due to the ability of the fungus to produce an acidic environment in order to make the nutrient of the culture medium available. As side effect, the organic acid produced by the fungus can partially dissolve the chitosan-based aerogels and use it as growth substrate. The functionalization with silver provided a more effective antimycotic affect. Indeed, heavy metals are known for their toxicity on microorganisms and the addition of silver to the chitosan solution provided the aerogels with antifungal property.

4.3 Tests in polluted environments

The aerogels were exposed to polluted environments to check their adsorption performances towards the selected pollutants. The exposure was performed using an excess of pollutants compared to the limit values suggested in a museum environment to speed the efficacy tests and check the adsorption capacity of the aerogels. It is worth stressing that the recommended levels of gaseous pollutants in museum environments evolved over time in that limits were lowered and other pollutants were included. The first specifications on pollutant limit levels were developed

in the UK in the 70s and in the USA in the 80s mainly focusing on archival records protection. Many heritage institutions adopted the specifications introduced in UK and USA [179]. Hereafter a table with the maximum pollutants' levels recommended by published specifications from Jean Tétreault 2018 is exposed (table 7), to give an overview of the limit values specified by different institutions (table 8) for some of the most dangerous pollutants in museum environments.

Table 7. Name of the published pollutant specifications considered by Tétreault.

PUBLISHED POLLUTANT SPECIFICATIONS	
BS 5454	Recommendations for the Storage and Exhibition of Archival Documents [180]
Thomson 1978	Garry Thomson, scientific adviser to the Trustees and head of the Scientific Department at the National Gallery in London [181]
NBS 1983	National Bureau of Standards [182]
NRC 1986	National Research Council (NRC) - USA [183]
BS 5454 1989-2000	British Standards Institution (BSI) [184]
NISO 1995	National Information Standards Organization (NISO) [185]
UNESCO 1998	United Nations Educational, Scientific and Cultural Organization (UNESCO) [186]
NARA 2022	National Archives and Records Administration - USA [187]
PAS198 2012*	British Standards Institution – Publicly Available Specification [188]

Table 8. Maximum pollutant levels recommended by published specifications in μg/m3 (ppb).

POLLUTANTS	BS 5454 1977	Thomson 1978	NBS 1983	NRC 1986	BS 5454 1989-2000	NISO 1995	UNESCO 1998	NARA 2002	PAS198 2012*
Acetic acid								10 (4)	250 (100)
Formaldehyde								5 (4)	375 (300)

Formic acid								958 (500)
Nitrogen dioxide		10 (5.2)	5 (2.6)		10 (5.2)	19 (10)	1 (0.5)	5 (2.6)	19 (10)
Ozone		2 (1)	25 (12.5)	2 (1)		10 (10)	2 (1)	4 (2)	20 (10)
Reduced Sulphides									-10
Sulphur dioxide	50 (18.7)	10 (3.7)	1 (0.4)	1 (0.4)	10 (3.7)	27 (10)	1 (0.4)	2.7 (1)	2.7 (1)
Total supsended particles			75				75		

4.3.1 Aerogels weight gain

The adsorption properties of the prepared aerogels were investigated by studying their interactions with aldehydes and organic acids, as acetaldehyde and acetic acid, that were selected as representative pollutants. The chitosan-based materials were exposed to a certain amount of pollutant in a sealed vessel, their weight gain was monitored and they were characterized by infrared spectroscopy. The weight gain values for all tested aerogels are presented in bar charts, combing the results obtained during the exposure to the pollutant with those obtained during the desorption process. The weight gain procedure was described in paragraph 3.6.1.

The first aerogels tested were those obtained from an A.A. solution. As stated previously, these tests were carried out to study the physical interaction between absorbents and volatile organic compounds, which is why A.A. was used also whit not functionalised aerogels. Organic acids, in fact, shouldn't interact chemically with chitosan and the functionalisation of the aerogels was conducted in order to make the systems able to chemically interact with both organic acids and acetaldehydes that were chosen as pollutants for this study.

The adsorption tests conducted by weight gain measurements were carried out on the aerogels obtained from A.A. solutions added with chitosan (Chit A.A.) as such and functionalised with Ag NPs, obtained from O.A. solutions added with chitosan (Chit O.A.) and obtained from S.A. solutions as such and functionalized with A. NPs and C.C. (Chit S.A.).

The weight gain % values of all the aerogels during their exposure to acetic acid resulted rather high. The increase in weight of the aerogels during the exposure to the pollutants is strictly related to the porosity of the system.

The weight gain measures were carried on using chitosan-based aerogels obtained from O.A. and S.A.. The different formulations were compared to study the differences in adsorption and retention capacity during and after the exposure respectively according to the different concentration in dissolution agent and chitosan.

The retention capacity was considered since it determines the pollutant released after the aerogel saturation thus taken into account the amount of physisorbed pollutant.

The retention capacity has also to be considered since it determines the pollutant released after the aerogel saturation thus taken into account the amount of physisorbed pollutant. The Chit S.A. 1H aerogels gave the best results with regard to both the adsorption during the exposure to acetic acid and the retention during the desorption treatment.

The aerogels obtained from a S.A. solution added with chitosan Chit S.A. 1H were then selected for the following tests with acetic acid and aldehydes (acetaldehydes and formaldehydes).

4.4 Aerogels chemical characterization

ATR-FTIR analysis were carried out on the aerogels after their exposure to the pollutants and the desorption treatment to avoid any interference of the physisorbed pollutant and to check its chemisorbed part. The aerogels interaction with acetaldehyde and acetic acid was studied by means of ATR-FTIR since aldehydes can be chemically adsorbed by polymeric amines such as chitosan via a reaction that leads to the formation of a Schiff base [155] whereas organic acids can be adsorbed by the fillers added to the chitosan matrix [170][171][172]. A comparison of the ATR-FTIR spectra of the aerogels as such with that of the same aerogel after its exposure to the pollutant and the desorption process was made for every aerogel, to check any differences that can be attributed to a chemical reaction with the VOCs.The first study of the chemisorption of chitosan towards aldehydes was carried out using aerogels obtained from an A.A. solution added with chitosan. ATR-FTIR analysis were carried out on the aerogels before their exposure to acetaldehyde (as such) and after 5h and 24h from the beginning of the desorption process. The main peaks associated to the chemisorption of aldehydes were identified and the modification of their intensity was used to monitor the adsorption capacity of the aerogels.

As previously described, to enhance the mitigation efficacy of the aerogels towards organic acids such as acetic acid, the aerogels were functionalized with A.NPs and C.C. particles.

The presence of new bands that indicate the formation of acetate forms and thus a chemical interaction between the filler and the pollutant.

The ATR-FTIR analysis on the aerogels functionalized with alkaline particles also confirmed a chemical interaction of the absorber with the pollutant.The results obtained from the ATR-FTIR analysis carried out on

the aerogels after their exposure to acetic acid, acetaldehyde and formaldehyde make it possible to confirm that a chemisorption of the selected pollutants by the developed systems occurred.

4.5 Coupon analysis

Among all the materials, the most sensitive to indoor pollutants turned out to be the metals and alloys whose corrosion products are, in fact, the most frequently studied [174]. Pollutants concentration limits for the safe storage and exhibition of art objects proposed in the literature can change according to the environment assessed and to the specific sensitivity of the materials, thus no explicit numbers are available. A relatively universal determination and estimation of indoor corrosivity can be made according to the ISO 11844 standard [2] which introduced corrosivity categories of indoor atmospheres on the basis of the corrosion rate. The corrosivity categories are ideally determined by measurement of the corrosion attack on standard specimens but may also be estimated by other procedures based on the knowledge of humidity, temperature and pollution conditions described in the standard. This standard thus enables to estimate the corrosivity category according to the environment conditions (i.e. type of indoor atmospheric environment, temperature, RH, etc.) and the corrosivity categories can be used to describe the quality of atmosphere from the perspective of materials other than metals.

Accurate monitoring of corrosion rates in any environment is critical when viewed in terms of the maintenance and repair costs associated with material degradation. Test coupons provide an inexpensive means of on-

line monitoring that allow to effectively measure the corrosivity within an environment.

The comparison of the ART-FTIR spectra along with the pictures of the coupons surface collected after their exposure to the pollutants, in the presence of some of the produced aerogels and without them, is a useful tool to check, in an easy and quick way, the effectiveness of the aerogels in mitigating the pollutant and in protecting the objects.

Observing the ATR-FTIR spectra in comparison, was noted, especially with regard to the copper alloy coupons, a clear difference in the intensity of the bands related to the corrosion products. Since, in every case, the bands intensity appeared lower for the spectra of the coupons exposed in the presence of the absorber, we can conclude that a mitigation of the pollutants inside the vessels because of the aerogels occurred.

The corrosion products revealed in the coupons surface were not just associated with the presence of the pollutant like formate and acetate but were also related to humidity and other pollutants present in the vessels at the time of the pollutant insertion. Indeed, it was not possible to choose a band intensity to take as a reference to compare the mitigation efficiency of the aerogels towards the selected pollutants because of the bands overlay and the differences in the spectra of repeated tests.

Metal coupons were also used as passive sampling devices to check the chitosan-based aerogel efficiency in mitigating the pollutants concentration in real environments. An Oddy test was carried out to check the possible modification of the atmosphere caused by the pollutants off-gassed from a wooden crates used to storage works of art using three different kind of coupons: lead coupons, copper alloy coupons and silver alloy coupons.

One disk for each alloy was put inside the crate and the other one outside the crate in the same room. Comparing the ATR-FTIR spectra collected analysing the surface of the silver alloy coupons exposed inside and outside the crate in the same room, was possible to observe a clear difference in the intensity of the bands related to the corrosion products. These last tests gave evidence of the corrosion power of the pollutants emitted from a storage crate towards metal objects and thus of the danger related even to the storage units specifically developed for art objects.

5 Conclusions and outlooks

The aim of the PhD AMAART Project was to contribute to the development of materials and approaches for an effective Preventive Conservation during storage and exhibition of art objects. Grant a safe environment for the multitude of art objects is a highly demanding goal and it is fundamental for a long-term preservation of billions of objects collected in museum, library and archive storages. For a correct conservation of the art works, the Preventive Conservation entails the monitoring and adjusting of the museum environments.

Within the AMAART Project, performed in the CNR-ISMN Research group in the framework of the H2020 APACHE project, chitosan-based aerogels were developed as passive adsorbers for the mitigation of pollutants concentration in museum indoor environment. The research activities were first focused on the development of chitosan adsorbers with a high surface area, a good porosity and a good structure, using different starting solution to be freeze-dried. The morphological characterization of the structure of the aerogels, carried out by means of FE-SEM, showed that a good porosity was reached for all the aerogels produced. The chitosan-based aerogels were functionalised with different fillers to enhance their chemisorption efficacy towards organic acid further to aldehydes and to enhance their antifungal properties. The adsorption and retention capacity of the aerogels was investigated monitoring the weight gain of the developed systems, during and after the exposure to the selected pollutants.

ATR-FTIR analysis were carried out to verify the chemical interaction of the aerogels with the pollutants.

Tests with metal coupons were also conducted to check the effectiveness of the aerogels in mitigating the pollutant and thus protect the art objects.

The results, obtained by means of the morphological and chemical-physical analysis carried out within the tests, were meant to select the best suitable aerogel.

A novel tool for a cheap mitigation of aggressive species in museum environment was developed, based on the results obtained testing and analyzing the aerogels produced during this research activity.

It is worth noting that the adsorbing system produced has very positive properties in addition to the adsorption and chemisorption capacity towards some of the most aggressive pollutants, such as sustainability, safety, low cost, ease of use.

In addition, the aerogels are easy to handle and can be easily put in the exhibition crates without being noticed too much.

This easy to use, cheap and green system developed at CNR-ISMN within the APACHE Project can be easily produced in larger amounts than that produced till now in laboratory and used as an efficient tool for the Preventive Conservation in museum, archives and libraries.

In parallel with the study and the development of the chitosan-based aerogels, the chemical, morphological and structural properties of the sensing materials, that have been developed by the CNR-ISM Research Group in collaboration with CNR-ISMN Research Group within the APACHE Project, were investigated during their development and after the tests. The analysis of the metal tracks 'surface helped to understand the results obtained by the CNR-ISM during the exposure of the sensors in tailored polluted environments. A different behavior of each sensor according to the metal they were composed of and the pollutant they were exposed to was, indeed, revealed.

This work has been carried out within the APACHE project funded by the European Union's Horizon 2020 Research and Innovation Programme under the grant agreement no. 814496.

6 Bibliography

[1] C.M. Grzywacz, *Monitoring for gaseous pollutants in museum environments-Tools for Conservation*, Getty Publications,Los Angeles, 2006.

[2] C. J. Weschler, Changes in indoor pollutants since the 1950s, *Atmospheric Environment*, 43, 2009, 153–169.

[3] J. Kim, S. Kim, K. Lee, D. Yoon, J. Lee, D. Ju, Indoor aldehydes concentration and emission rate of formaldehyde in libraries and private reading rooms, *Atmospheric* Environment, 71, 2013, 1-6.

[4] D. Grosjean, A. H. Miguel, T. M. Tavares, Urban air pollution in Brazil: acetaldehyde and other carbonyls Atmospheric Environment, 24B, 1990, 101-106.

[5] A. Schieweck , B. Lohrengel , N. Siwinski , C. Genning , T. Salthammer, Organic and inorganic pollutants in storage rooms of the Lower Saxony State Museum Hanover, Germany, *Atmospheric Environment*, 39, 2005, 6098–6108.

[6] Museums Australia Victoria. The Effects of Storage and Display Materials on Museum Objects.
http://www.mavic.asn.au/assets/Info_Sheet_7_Effects_of_Storage.pdf
(accessed March 2020).

[7] Dafni A. Missia, E. Demetrio, N. Michael, E.I. Tolis, J.G. Bartzis, Indoor exposure from building materials: A field study, *Atmospheric Environment*, 44, 2010, 4388-4395.

[8] B. Clarisse, A.M. Laurent, N. Seta, Y. Le Moullec, A. El Hasnaoui, I. Momas, Indoor aldehydes: measurement of contamination levels and

identification of their determinants in Paris dwellings, *Environmental Research*, 92, 2003, 245–253.

[9] A. Baez, H. Padilla, R. Garcia, Ma. del Carmen Torres, I. Rosas, R. Belmont, Carbonyl levels in indoor and outdoor air in Mexico City and Xalapa, Mexico, *The Science of the Total Environment*, 302, 2003, 211–226.

[10] C. Marchand, B. Bulliot, S. Le Calve´, Ph. Mirabel, Aldehyde measurements in indoor environments in Strasbourg (France), *Atmospheric Environment* 40, 2006, 1336–1345.

[11] H.N. Knudsen, U.D. Kjaer, P.A. Nielsen, P. Wolkoff, Sensory and chemical characterization of VOC emissions from building products: impact of concentration and air velocity, *Atmospheric Environment*, 33, 1999, 1217—1230.

[12] H. Wang, G. C. Morrison, Ozone-Initiated Secondary Emission Rates of Aldehydes from Indoor Surfaces in Four Homes, *Environ. Sci.Technol.*, 40, 2006, 5263-5268.

[13] C. J. Weschler, A. T. Hodgson, J. D. Wooley, Indoor Chemistry: Ozone, Volatile Organic Compounds, and Carpets, *Environ. Sel. Technol*., 26, 1992, 2371-2377.

[14] J. Zhang, Q. He, P. J. Lloy, Characteristics of Aldehydes: Concentrations, Sources, and Exposures for Indoor and Outdoor Residential Microenvironments, *Environ. Sci. Technol*., 28, 1994, 146-152.

[15] J. P. Conkle, B. J. Camp, B. E. Welch, Trace Composition of Human Respiratory Gas, *Archives of Environmental Health: An International Journal*, 30:6, 1975, 290-295.

[16] J. Zhang, W. E. Wilson, P. J. Lloy, Indoor Air Chemistry: Formation of Organic Acids and Aldehydes, *Environ. Sci. Technol.*, 28, 1994,1975-1982.

[17] M. Risholm-Sundman, M. Lundgren, E. Vestin, P. Herder, Emissions of acetic acid and other volatile organic compounds from different species of solid wood, *Holz als Roh-und Werkstoff* , 56, 1998, 125–129.

[18] S. J. Smith, J. van Aardenne, Z. Klimont, R. J. Andres, A. Volke, S. Delgado Arias, Anthropogenic sulfur dioxide emissions: 1850–2005, *Atmos. Chem. Phys.*, 11, 2011, 1101–1116.

[19] World Health Organization. Regional Office for Europe. Air quality Guidelines: particulate matter, ozone, nitrogen, dioxide and sulfur dioxide, Global Update 2005, *Copenhagen : World Health Organization, Europe, 2006.*

[20] H. A. Ankersmita, N. H. Tennent, S. F. Watts, Hydrogen sulfide and carbonyl sulfide in the museum environment—Part 1, *Atmospheric Environment*, 39, 2005, 695–707.

[21] P. Brimblecombe, D. Shooter, A. Kaur, Wool and Reduced Sulphur Gases in Museum Air, *Studies in Conservation*, 37, 1992, 53-60.

[22] N. L. Gilbert, D. Gauvin, M. Guay, M. E. Héroux, G. Dupuis, M. Legris, C. C. Chan, R. N. Dietz, B. Lévesque, Housing characteristics and indoor concentrations of nitrogen dioxide and formaldehyde in Quebec City, Canada, *Environmental Research*, 102, 2006, 1-8.

[23] WHO, 1997. Nitrogen Oxides. Environmental Health Criteria 189. World Health Organization, International Programme on Chemical Safety, Geneva, Switzerland.

[24] J. S. Kiurski, I. B. Oros, V. S. Kecic, I. M. Kovacevic, S. M. Aksentijevic, The temporal variation of indoor pollutants in photocopying shop, *Stoch Environ Res Risk Assess*, 30, 2016, 1289–1300.

[25] Jos Lelieveld, Frank J. Dentener, What controls tropospheric ozone?, *Journal of Geophysical Research*, 105, 2000, 3531-3551.

[26] R.J. Allen, R.A. Wadden, E.D. Ross, Characterization of Potential Indoor Sources of Ozone, *American Industrial Hygiene Association Journal*, 39, 1978, 466-471.

[27] M. R. Raychaudhuri and P.Brimblecombe Formaldehyde Oxidation and Lead Corrosion, Studies in Conservation, 45:4, 2000, 226-232.

[28] J. Tétreault, A.-L. Dupont, P. Bégin, S. Paris, The impact of volatile compounds released by paper on cellulose degradation in ambient hygrothermal conditions, *Polymer Degradation and Stability*, 98, 2013, 1827-1837.

[29] D. L. A. De Faria, A. Cavicchioli, T. S. Puglieri, Indoors lead corrosion: reassessing the role of formaldehyde, *Vibrational Spectroscopy*, 54, 2010, 159-163.

[30] T. S. Puglieri, D. L.A. de Faria, A. Cavicchioli, Indoor corrosion of Pb: Effect of formaldehyde concentration and relative humidity investigated by Raman microscopy, *Vibrational Spectroscopy*, 71, 2014, 24-29.

[31] Mary F. Striegel, The effects of gas phase formaldehyde on selected inorganic materials found in museums, *Objects Specialty Group Postprints*, 1, 1991, 1-12.

[32] E. Cano, J. M. Bastidas, Effect of relative humidity on copper corrosion by acetic and formic acid vapors, *Canadian Metallurgical Quarterly*, 41, 2002, 327-336.

[33] C. Leygraf, I. O. Wallinder, J. Tidblad, T. Graedel, *Atmospheric Corrosion*, Wiley, New York, 2016, 2a ed.

[34] C.M. Johnson, C. Magnus, Vibrational Sum Frequency and Infrared Reflection/Absorption Spectroscopy Studies of the Air/Liquid and Liquid/Metal Interfaces, *Meet. Abstr*., 2, 2007, 827.

[35] A.-L. Dupont & J. Tetreault, Cellulose Degradation in an Acetic Acid Environment, *Studies in Conservation*, 45:3, 2000, 201-210.

[36] Edwin L. Williams, Eric Grosjean, Daniel Grosjean, Exposure of Artists' Colorants to Airborne Formaldehyde, *Studies in Conservation*, 37, 1992, 201-210.

[37] O. Vilanova, B. Sanchez, M.C. Canela, Proceedings of the 4th International Congress Science and Technology for the Conservation of Cultural Heritgae (Technoheritage 2019), Seville, Spain, 26-30 March 2019. Interaction of heritage pigments with volatile organic compounds (VOCs). A laboratory study, *Science and Digital Technology for Cultural Heritage, Interdisciplinary Approach to Diagnosis, Vulnerability, Risk Assessment and Graphic Information Models, 2020 Taylor and Francis Group, London*, 390-394.

[38] M. Malagodi, C. Milanese, M. Licchelli, P. Cofrancesco, S. Bottigliero and T. Rovetta, Alteration processes of pigments exposed to acetic and formic acid vapors, *2017 IEEE International Conference on Environment and Electrical Engineering and 2017 IEEE Industrial and Commercial Power Systems Europe (EEEIC / I&CPS Europe)*, Milan, 2017, 1-6.

[39] N. De Laet, S. Lycke, J. Van Pevenage, L. Moens, P. Vandenabeele, Investigation of pigment degradation due to acetic acid vapours: Raman spectroscopic analysis, *European Journal of Mineralogy*, 25 (5), 2013, 855–862.

[40] A. Kenyon, Notes on the effects of the atmosphere on the shells of mollusca, *Proceedings of the Royal Society of Tasmania for 1896*, 1897, 88.

[41] L.S.G Byne, The corrosion of shells in cabinets, *Journal of Conchology*, 9, 899, 172–178.

[42] J. R. Nicholls, Deterioration of shells when stored in oak cabinets, *Chemistry and Industry,* 53, 1934, 1077–1078.

[43] A. Boccia Paterakis, Efflorescence testing on pottery, *The ceramics cultural heritage: proceedings of the international symposium "The Ceramics Heritage" of the 8th CIMTEC-World Ceramics Congress and Forum on New Materials*, *TECHNA*, 1994.

[44] A. Boccia Paterakis, M. Steiger Salt efflorescence on pottery in the Athenian Agora: A closer look, *Studies in Conservation*, 60:3, 2015, 172-184.

[45] L. T. Gibson, B. G. Cooksey, D. Littlejohn, K. Linnow, M. Steiger, N. H. Tennent, The Mode of Formation of Thecotrichite, a Widespread Calcium Acetate Chloride Nitrate Efflorescence, *Studies in Conservation*, 50:4, 2005, 284-294.

[46] M. D. King, F N Fisher, K. C. Thompson, A. D. Ward, Reactions on atmospheric mineral aerosol, *Lasers for Science Facility Programme – Chemistry*, Central Laser Facility Annual Report 2004/2005.

[47] M. Nockert, T. Wadsten, Storage of archaeological textile finds in sealed boxes, *Studies in Coinservation*, 23, 1978, 38-41.

[48] L. Robinet, K. Eremin, B. Cobo del Arco, L. T. Gibson, A Raman spectroscopic study of pollution-induced glass deterioration, *Journal of Raman Spectroscopy*, 35, 2004, 662–670.

[49] L. Robinet, S. Fearn, K. Eremin, Understanding glass deterioration in museum collections: a multi-disciplinary approach, *14th Triennial Meeting the Hague Preprints*, vol. I, ICOM committee for conservation, 2005.

[50] K. Eremin, B. Cobo del Arco, L. Robinet, L. T. Gibson, Conservation and analysis of deteriorating nineteenth and twentieth-century British glass in the National Museums of Scotland, Annales du 16ème Congrès International d'Etude Historique du Verre, London. *International d'Etude Historique du Verre, Nottingham*, UK, pp. 380-385, 2005.

[51] L. Jordan, L. H. Grenell, H.K. Herschman, Tarnish resisting silver alloys, Technologic Papers of the Bureau of Standards, No. 348, Part of Vol. 21, 1927.

[52] S. Lilienfeld, C. E. White, A study of the reaction between hydrogen sulfide and silver, *J. Am. Chem. Soc.* 52, 3, 1930, 885–892.

[53] H. Fischmeister, J. Drott, Reaction rate and growth forms of reaction product in the system Ag-H_2S, *Acta Metallurgica*, 7, 1959.

[54] H. E. Bennett, R. L. Peck, D. K. Burge, J. M. Bennett, Formation and Growth of Tarnish on Evaporated Silver Films, *Journal of Applied Physics*, 40, 1969, 3351.

[55] J. P. Franey, G. W. Kammlott, T. E. Graedel, The corrosion of silver by atmospheric sulfurous gases, Corrosion Science, 25, 1985, 133-143.

[56] T. E. Graedel, J. P. Franey, G. J. Gualtieri, G. W. Kammloty, D. L. Malm, On the mechanism of silver and copper sulfidation by atmospheric H_2S and OCS, *Corrosion Science*, 25, 1985, 1163-1180.

[57] L. Volpe, P. J. Peterson, The atmospheric sulfidation of silver in a tubular corrosion reactor, *Corrosion Science*, 29, 1989, 1179-1196.

[58] C. Hillman, J. Arnold, S. Binfield, J. Seppi, Silver and sulfur: case studies, physics, and possible solutions, SMTA International, 2007, DfR Solutions, College Park, MD, http://www.dfrsolutions.com/uploads/publications/2007_10_silver_and_sulfur.pdf .

[59] M. Watanabe, A. Hokazono, T. Handa, T. Ichino, N. Kuwaki, Corrosion of copper and silver plates by volcanic gases, *Corrosion Science*, 48, 2006, 3759-3766.

[60] M. Reid, J. Punch, C. Ryan, L. F. Garfias, S. Belochapkine, J. P. Franey, G. E. Derkits, W. D. Reents, Microstructural development of copper sulfide on copper exposed to humid H_2S, *Journal of Electrochemical Society*, 154, 2007, C209-C214.

[61] G. D. Smith, Robin J.H. Clark, The role of H_2S in pigment blackening, *Journal of Cultural Heritage*, 3, 2002, 101–105.

[62] G. D. Smith, A. Derbyshire, R. J. H. Clark, In situ Spectroscopic Detection of Lead Sulphide on a Blackened Manuscript Illumination by Raman Microscopy, *Studies in Conservation*, 47, 2002, 250-256.

[63] N. Blades, T. Oreszczy, B. Bordass, M. Cassar, Guidelines on pollution control in heritage building, *The Council for Museums, Archives and Libraries*, 2000.

[64] G. Pavlogeorgatos, Environmental parameters in museums, *Building and Environment* 38, 2003, 1457–1462.

[65] S. E. Schwartz, Both Sides Now: The Chemistry of Clouds a., *Annals of the New York Academy of Sciences*, 502(1), 1987, 83-144.

[66] J. Tidblad, *Atmospheric corrosion of heritage metallic artefacts: processes and prevention*, Elsevier Ltd, 2013, p. 37-52.

[67] J. Tidblad, T. E. Graedel, Gildes model studies of aqueous chemistry. III. initial sot-induced atmospheric corrosion of copper, *Corrosion Science*, 38, 1996, 2201-2224.

[68] W. H. J. Vernon, A laboratory study of the atmospheric corrosion of metals. Part I.—The Corrosion of copper in certain synthetic atmospheres, with particular reference to the influence of sulphur dioxide in air of various relative humidity, *Transactions of the Faraday Society*, 27, 1931.

[69] S. Oesch, M. Faller, Environmental effects on materials: the effect of the air pollutants SO_2, NO_2, no and O_3 on the corrosion of copper, zinc and aluminium. A short literature survey and results of laboratory exposures, *Corrosion Science*, 39, 1997, 1505-l 530.

[70] R. Ericsson, T. Sydberger, Corrosion Products Formed on Copper exposed to humid SO_2-containing atmospheres, *Materials and Corrosion* 28, 1977, 755-757.

[71] Peter Eriksson, Lars-Gunnar Johansson, Helena Strandberg, Initial Stages of Copper Corrosion in Humid Air Containing SO_2 and NO_2, *Journal of Electrochemical Society* 140, 1993, 53-59.

[72] Q. Qu, C. Yan, Y. Wana, C. Cao, Effects of NaCl and SO_2 on the initial atmospheric corrosion of zinc, *Corrosion Science*, 44, 2002, 2789–2803.

[73] Svensson and L. G. Johansson, The temperature-dependence of the SO2-induced atmospheric corrosion of zinc; a laboratory study, *Corrosion Science*, 38, 1996, 2225-2233.

[74] J. E. Svensson and L. G. Johansson, A laboratory study of the effect of ozone, nitrogen dioxide, and sulfur dioxide on the atmospheric corrosion of zinc, *Journal of Electrochemical Society*, 140, 1993, 2210.

[75] D. J. Spedding, R. P. Rowlands, J. E. Taylor, Sorption of sulphur dioxide by indoor surfaces III.†—Leather, J*ournal of applied Chemistry*, 20, 1970, 226.

[76] G. Vyskočilová, M. Ebersbach, R. Kopecká, L. Prokeš, J. Příhoda, Model study of the leather degradation by oxidation and hydrolysis, *Heritage Science* 7, 2019, 26.

[77] P. Brimblecombe, D. J. Bowden, Sulphur distribution in parchment and leather exposed to sulphur dioxide, *Journal of the Society of Leather Technologists and Chemists*, 84, 2000, 177-186.

[78] Edwin L. Williams, Daniel Grosjean, Exposure of deacidified and untreated paper to ambient levels of sulfur dioxide and nitrogen dioxide: nature and yields of reaction products, *Journal of the American Institute for Conservation*, 31, 1992, 199-212.

[79] F. Lyth Hudson., W. D. Milner B, Atmospheric Sulphur and the durability of paper, *Journal of the Society of Archivists*, 2:4, 1961, 166-167.

[80] W. H. Langwell, Measurement of the effects of air pollution on paper documents, *Journal of the Society of Archivists*, 5:6, 1976, 372-373.

[81] Arthur E. Kimberly, Deteriorative effect of sulphur dioxide upon paper in an atmosphere of constant humidity and temperature, *Bureau of Standards Journal of Research*, 8, 1932, 159-171.

[82] Myoung Nam Kim, Bo A Lim, Eun Jeong Shin, Sun Myung Lee, Damage characteristics of Korean traditional textiles by sulfur dioxide, *Journal of Conservation Science*,28, 2012, 321-328.

[83] S.H. Zeronian, K.W. Alger, S.T. Omaye, Effect of Sulfur Dioxide on the Chemical and Physical Properties of Nylon,*Textile Research* Journal, 43, 1973, 228–237.

[84] V. S. Salvin, Effect of Air Pollutants on Dyed Fabrics, *Journal of the Air Pollution Control Association*, 13:9, 1963, 416-455.

[85] Ana Alebic-Juretic, Duska Sekulic-Cikovic, The Impact of Air Pollution on the Paintings in Storage at the Museum of Modern and Contemporary Art, Rijeka, Croatia, *Studies in Conservation*, 54, 2009, 49-57.

[86] M. Maguregui, U. Knuutinen, I. Martínez-Arkarazo, K. Castro, J. M. Madariaga, Thermodynamic and Spectroscopic Speciation to Explain the Blackening Process of Hematite Formed by Atmospheric SO_2 Impact: The Case of Marcus Lucretius House (Pompeii), *Analytical Chemistry*, 83, 2011, 3319–3326.

[87] S. Aze, J.-M. Vallet, M Pomey, A. Baronnet, O. Grauby, Red lead darkening in wall paintings: natural ageing of experimental wall paintings versus artificial ageing tests, *European Journal of Mineralogy*, 19, 2007, 883–890.

[88] Z.C.Kang, Laura Machesky, H.A.Eick, L.Eyring, The solvolytic disproportionation of mixed-valence compounds: III. Pb_3O_4, *Journal of Solid State Chemistry*, 75, 1988, 73-89.

[89] Edwin L. Williams, II, Eric Grosjean, Daniel Grosjean, Exposure of Artists' Colorants to Sulfur Dioxide, *Journal of the American Institute for Conservation*, 32, 1993, 291-310.

[90] Juan Luis Pérez Bernal, Miguel Angel Bello, Modeling sulfur dioxide deposition on calcium carbonate, *Industrial & Engineering Chemistry Research*, 42, 2003, 1028-1034.

[91] P. Elfving, The initial steps in the air pollution induced deterioration of calcareous stone, *In Proceedings of the 1995 LCP congress*, 1995, 421-427.

[92] K. L. Gauri, R. Popli, A. C. Sarma, Effect of relative humidity and grain size on the reaction rates of marble at high concentrations of SO_2, *Durability of Building Materials*, 1, 1982, 209.

[93] E. C. Spiker, V. J. Comer, R. P. Hosker, S. I. Sherwood, Dry deposition of SO_2 on limestone and marble: Role of humidity, *eds. Proceedings of the 7th International Congress on Deterioration and Conservation of Stone*, 1992, 397-406.

[94] J. E. Svensson, L. G. Johansson, A laboratory study of the effect of ozone, nitrogen dioxide and Sulphur dioxide on the atmospheric corrosion of zinc, Journal of Electrochemical Society, 140, 1993, 2210.

[95] J.G. Castaño, D. de la Fuente, M. Morcillo, A laboratory study of the effect of NO_2 on the atmospheric corrosion of zinc, Atmospheric Environment, 41, 2007, 8681–8696.

[96] H. Kim, Corrosion process of silver in environments containing 0.1 ppm H_2S and 1.2 ppm NO_2, *Materials and Corrosion*, 54, 2003, 243–250.

[97] M. Seo, I. Sawamura, N. Sato, Proceedings of the 1st Inter. Symp. on Corrosion of Electronic Materials, *The Electrochemical Society Proceedings*, 1991, 91-2.

[98] B. I. Rickett, J. H. Payer, Composition of Copper Tarnish Products Formed in Moist Air with Trace Levels of Pollutant Gas: Sulfur Dioxide and Sulfur Dioxide/Nitrogen Dioxide, *Journal of Electrochemical Society*, 142, 1995, 11.

[99] Hisayoshi Takazawa, Effect of NO_2 on the Atmospheric Corrosion of Metals, *Boshoku Gijutsu*, 34, 1985, 612-617.

[100] D. Grosjean, E. Grosjean, E. l. Williams, Fading of artists' colorants by a mixture of photochemical oxidants, *Atmospheric Enviromnent*, 27A, 1993, 765 772.

[101] P. M. Whitmore, G. R. Cass, The fading of artists' colorants by exposure to atmospheric nitrogen dioxide, *Studies in Conservation*, 34, 1989, 85-97.

[102] H. Jerosch, B. Lavedrine, J.-C. Cherton, The use of size exclusion chromatography (sec) for the evaluation of paper degradation caused by nitrogen oxides in comparison with other methods, *Studies in Conservation*, 47, 2002, 108-113.

[103] M. N. Kim, B. A Lim, S. Kim, S. M. Lee, Damage Characteristics of Korean Traditional Textiles by Nitrogen Dioxid e (NO_2) Concentrations, *Journal of Conservation Science* Vol.29, No.3, pp197-207 (2013).

[104] S. W. Massey, The effects of ozone and NO_x on the deterioration of calcareous stone, *The Science of the Total Environment*, 227, 1999, 109-121.

[105] A. Sarmiento, M. Maguregui, I. Martinez-Arkarazo, M. Angulo, K. Castro, M. A. Olaz´abal, L. A. Fernández, M. D. Rodriguez-Laso, A. M. Mujika,3 J. Gómez, J. M. Madariaga, Raman spectroscopy as a tool to diagnose the impacts of combustion and greenhouse acid gases on properties of Built Heritage, *Journal of Raman Spectroscopy*, 39, 2008, 1042–1049.

[106] A. Vykydalová, Z. Cibulková, K. Čížová, K. Vizárová, P. Šimona, Degradation of bees wax by NOx pollution and UV light studied by DSC and FTIR measurements, *Thermochimica Acta*, 689, 2020, 178606.

[107] D. W. Rice, P. Peterson, E. B. Rigby, P. B. P. Phipps, R. J. Cappell, R. Tremoureux, Atmospheric Corrosion of Copper and Silver, *Journal of The Electrochemical Society*, 128, 1981, 275.

[108] J. Onye, G. S. Frankel, Effects of NaCl, SO_2, NH_3, O_3, and ultraviolet light on atmospheric corrosion of Zn, *Materials and Corrosion*, 71, 2020, 9–20.

[109] T. Aastrup, M. Wadsak, VC. Leygraf, M. Schreiner, In Situ Studies of the Initial Atmospheric Corrosion of Copper Influence of Humidity, Sulfur Dioxide, Ozone, and Nitrogen Dioxide, *Journal of The Electrochemical Society*, 147, 2000, 2543-2551.

[110] S. Zakipour, J. Tidblad, C. Leygraf, Atmospheric Corrosion Effects of SO_2 and O_3 on Laboratory-Exposed Copper, Journal of the Electrochemical Society, 142, 1995, 757.

[111] Z. Y. Chen, D. Liang, G. Ma, G. S. Frankel, H. C. Allen & R. G. Kelly, Influence of UV irradiation and ozone on atmospheric corrosion of bare silver, *Corrosion Engineering, Science and* Technology, 45, 2010, 169.

[112] R. Wiesinger, I. Martina, Ch. Kleber, M. Schreiner, Influence of relative humidity and ozone on atmospheric silver corrosion, *Corrosion Science*, 77, 2013, 69–76.

[113] K. Drisko, G. R. Cass, P- M. Whitmore, Fading of artists' pigments due to atmospheric ozone, 2-3, 1985, 66-87.

[114] P. M. Whitmore, G. R. Cass, J. R. Druzik, The Ozone Fading of Traditional Natural Organic Colorants on Paper, *Journal of the American Institute for Conservation*, 26, 1987, 45-57.

[115] D. Grosjean, P. M. Whitmore, C. P. De Moor, G. R. Cass, Fading of Alizarin and Related Artists' Pigments by Atmospheric Ozone: Reaction Products and Mechanisms, *Environmental Science Technology*, 1987, 21, 635-643.

[116] D. Grosjean, P. M. Whitmore, C. P. De Moor, G. R. Cass, Ozone Fading of Natural Organic Colorants: Mechanisms and Products of the Reaction of Ozone with Indigos, *Environmental Science Technology*, 22, 1988, 292-298.

[117] C. L. Shaver, G. R. Cass, Ozone and the Deterioration of Works of Art, *Environmental Science Technology*, 17, 1983, 748-752.

[118] D. Grosjean, P. M. Whitmore, C. P. De Moor, G. R. Cass, Ozone Fading of Organic Colorants: Products and Mechanism of the Reaction of Ozone with Curcumin, *Environmental Science Technology*, 22, 1988, 1357-1361.

[119] J. S. Rugg, Ozone Crack Depth Analysis for Rubber, *Analytical Chemistry*, 2 4, 1932.

[120] R. Cuthbertson, D. D. Dunnom, Cracking of rubber and GR-S in ozone - Effects of Temperature and Elongation Ozone Cracking, *Industrial and Engineering Chemistry*, 44:4, 1952.

[121] S. Kamarudd, A. H. Muhr, Investigation of Ozone Cracking on Natural Rubber, *Journal of Rubber Research*, 21, 2018, 73-93.

[122] M. Ryhl-Svendsen, J. Glastrup, Acetic acid and formic acid concentrations in the museum environment measured by SPME-GC/MS, *Atmospheric Environment*, 36, 2002, 3909-3916.

[123]https://www.environnement.it/94/33/CAIRCLIP_Sensori_Miniaturizzati_per_il_monitoraggio_dell-inquinamento_odorigeno.htm, 2019/06/21. (accessed March 2021).

[124] https://www.draeger.com/en-us_us/Applications/Tubes-Handbook, 2019/06/21. (accessed March 2021).

[125] B.Szulczynski, J, Gebicki, Currently Commercially Available Chemical Sensors Employed for Detection of Volatile Organic Compounds in Outdoor and Indoor Air, *Environments*, 4, 2017, 21.

[126]http://www.cwaller.de/english.htm?aircorr/e_aircorr1_plus.htm~information, 2019/06/21. (accessed March 2021).

[127] M. Kouril, T. Prosek, B. Scheffel, Y. degres, Corrosion monitoring in archives by the electrical resistance technique, *Journal of Cultural Heritage* 15, 2014, 99-103.

[128] H. A. Ankersmit, N. H. Tennent, F. Watts, Hydrogen sulphide and carbonyl sulphide in the museum environment– Part I, *Atmospheric Environment*, 39, 2005, 695-707.

[129]http://www.cwaller.de/english.htm?aircorr/e_aircorr1_plus.htm~information, 2019/06/21. (accessed April 2021).

[130] K. Popova, T. Prošek, Corrosion Monitoring in Atmospheric Conditions: A Review, *Metlas*, *12*, 2022, 171.

[131] H. A. Ankersmit, N. H. Tennent, F. Watts, Hydrogen sulphide and carbonyl sulphide in the museum environment– Part I, *Atmospheric Environment*, 39, 2005, 695-707.

[132] A.L. Dupont, J. Tetreault, Cellulose Degradation in an Acetic Acid Environment, Studies in Conservation, 45, 2000, 201-210.

[133] https://www.gradko.com/environmental/,2019/06/21. (accessed April 2021).

[134] Li, X.; Zhang, L.; Yan, Z.; Wang, P.; Yan, Y.; Ran, J.; Adsorption materials for volatile organic compounds (VOCs) and the key factors for VOCs adsorption process: A review, *Separation and Purification Technology* 235, 2020, 116213.

[135] Lingli Zhu, Dekui Shen, Kai Hong Luo, A critical review on VOCs adsorption by different porous materials: Species, mechanisms and modification methods, *Journal of Hazardous Materials*, 389, 2020, 122102.

[136] Faisal I. Khan, Aloke Kr. Ghoshal, Removal of Volatile Organic Compounds from polluted air, *Journal of Loss Prevention in the Process Industries*, 13, 2000, 527–545.

[137] Xueyang Zhang, Bin Gao, Anne Elise Creamer, Chengcheng Cao, Yuncong Li, Adsorption of VOCs onto engineered carbon materials: A review, *Journal of Hazardous Materials*, 338, 2017, 102-123.

[138] Chunyu Chen, Xiong Wang, Jian Zhang, Chaoqun Bian, Shuxiang Pan, Fang Chen, Xiangju Meng, Xiaoming Zheng, Xionghou Gao, Feng-Shou Xiao, Superior performance in catalytic combustion of toluene over

mesoporous ZSM-5 zeolite supported platinum catalyst, *Catalysis Today*, 258, 2015, 190-195.

[139] Rio Nugraha Putra, Young Haeng Lee, Entrapment of micro-sized zeolites in porous hydrogels: Strategy to overcome drawbacks of zeolite particles and beads for adsorption of ammonium ions, *Separation and Purification Technology*, 237, 2020, 116351.

[140] Xueyang Zhang, Bin Gao, Anne Elise Creamer, Chengcheng Cao, Yuncong Li, Adsorption of VOCs onto engineered carbon materials: A review, *Journal of Hazardous Materials*, 338, 2017, 102-123.

[141] Ikram Jarraya, Sophie Fourmentin, Mourad Benzina, Samir Bouaziz, VOC adsorption on raw and modified clay materials, Chemical Geology, 275, 2010, 1-8.

[142] D. Ricaurte Ortega & A. Subrenat Siloxane treatment by adsorption into porous materials, Environmental Technology, 30:10, 2009, 1073-1083.

[143] Netravali, Anil & Chabba, Shitij. (2003). Composites get greener. *Materials Today - MATER TODAY*. 6. 22-29. 10.1016/S1369-7021(03)00427-9.

[144] Cui Lai, Zhihong Wang, Lei Qin, Yukui Fu, Bisheng Li, Mingming Zhang, Shiyu Liu, Ling Li, Huan Yi, Xigui Liu, Xuerong Zhou, Ning An, Ziwen An, Xiaoxun Shi, Chongling Feng, Metal-organic frameworks as burgeoning materials for the capture and sensing of indoor VOCs and radon gases, Coordination Chemistry Reviews, 427, 2021, 213565.

[145] Duan, C., Yu, Y., Li, J. et al. Recent advances in the synthesis of monolithic metal-organic frameworks. Sci. China Mater. 64, 2021, 1305–1319.

[146] Sundararajan V. Madihally, Howard W.T. Matthew, Porous chitosan scaffolds for tissue engineering , *Biomaterials*, 20, 1999, 1133-1142.

[147] J. Lucas de Oliveira Arias, A. Schneider, J. A. Batista-Andrade, A. Alves Vieira, S.Souza Caldas, E. G. Primel, Chitosan from shrimp shells: A renewable sorbent applied to the clean-up step of the QuEChERS method in order to determine multi-residues of veterinary drugs in different types of milk, *Food Chemistry*, 240, 2018, 1243-1253.

[148] S. Roller, N. Covill, The antifungal properties of chitosan in laboratory media and apple juice *International Journal of Food Microbiology* 47, 1999, 67–77.

[149] L. Yien Ing, N. Mohamad Zin, A. Sarwar, H. Katas, Antifungal Activity of Chitosan Nanoparticles and Correlation with Their Physical Properties, *International Journal of Biomaterials* Volume, 2012, 632698.

[150] Mohamad M. Ayad, Nehal Salahuddin, Islam M. Minisy, Detection of some volatile organic compounds with chitosan-coated quartz crystal microbalance, *Designed Monomers and Polymers*, 17:8, 2014, 795-802.

[151] T. Wada, T. Uragami, Y. Matob, Chitosan-Hybridized Acrylic Resins Prepared in Emulsion Polymerizations and Their Application As Interior Finishing Coatings, *JCT Research*, 2, 2005, 577-592.

[152] N. Behary, A. Perwuelz, C. Campagne, D. Lecouturier, P. Dhulster, A.S. Mamede, Adsorption of surfactin produced from Bacillus subtilis using nonwoven PET (polyethylene terephthalate) fibrous membranes functionalized with chitosan, *Colloids and Surfaces B: Biointerfaces*, 90, 2012, 137–143.

[153] S. Nuasaen, P. Opaprakasit, P. Tangboriboonrat, Hollow latex particles functionalized with chitosan for the removal of formaldehyde from indoor air, *Carbohydrate Polymers*, 101, 2014, 179–187.

[154] L. Mohan V, S.M. Shiva Nagendra, M.P. Maiya, Photocatalytic degradation of gaseous toluene using self-assembled air filter based on chitosan/activated carbon/TiO_2, *Journal of Environmental Chemical Engineering* 7, 2019, 103455.

[155] Zhanyong Guo, Ronge Xing, Song Liu, Huahua Yu, Pibo Wang, Cuiping Lia, Pengcheng Lia, The synthesis and antioxidant activity of the Schiff bases of chitosan and carboxymethyl chitosan *Bioorganic & Medicinal Chemistry Letters*, 15, 2005, 4600–4603.

[156] Po-Hui Chen, Ya Hsi Hwang, Ting-Yun Kuo, Fang-Hsuan Liu, Juin-Yih Lai, Hsyue-Jen Hsieh, Improvement on the properties of chitosan membranes using natural organic acid solutions as solvents for chitosan dissolution, *Journal of medical and Biological Engineering*, 27(1), 2007, 23-28.

[157] Po-Hui Chen, Ting-Yun Kuo, Fang-Hsuan Liu, Ya-His Hwang, Ming-Hua Ho, Da-Ming Wang, Juin-Yih Lai, Hsyue-Jen Hsieh, Use of Dicarboxylic Acids to Improve and Diversify the Material Properties of Porous Chitosan Membranes, *J. Agric. Food Chem.*, 56, 2008, 9015–9021.

[158] C.K.S. Pillai, Willi Paul, Chandra P. Sharma, Chitin and chitosan polymers: Chemistry, solubility and fiber formation, *Progress in Polymer Science*, 34, 2009, 641–678.

[159] Magdolna Bodnar, John F. Hartmann and Janos Borbely, Preparation and Characterization of Chitosan-Based Nanoparticles, *Biomacromolecule*s 2005, 6, 2521-2527.

[160] Alain C. Pierre and Gérard M. Pajonk, Chemistry of Aerogels and Their Applications, *Chem. Rev.* 102, 11, 2002 4243–4266,

[161] Jun Sung Kim, Eunye Kuk, Kyeong Nam Yu, Jong-Ho Kim, Sung Jin Park, Hu Jang Lee, So Hyun Kim, Young Kyung Park, Yong Ho Park, Cheol-Yong Hwang, Yong-Kwon Kim, Yoon-Sik Lee, Dae Hong Jeong, Myung-Haing Cho, Antimicrobial effects of silver nanoparticles, *Nanomedicine: Nanotechnology, Biology and Medicine*, 3, 2007, 95-101,

ISSN 1549-9634, https://doi.org/10.1016/j.nano.2006.12.001.

[162] Suchomel P, Kvitek L, Panacek A, Prucek R, Hrbac J, Vecerova R, Comparative Study of Antimicrobial Activity of AgBr and Ag Nanoparticles (NPs). *PLoS ONE*, 17, 2015, 10(3): e0119202.

[163] Bui, V.K.H.; Park, D.; Lee, Y.-C. Chitosan Combined with ZnO, TiO_2 and Ag Nanoparticles for Antimicrobial Wound Healing Applications: A Mini Review of the Research Trends. Polymers, 9(1), 2017, 21.

[164] Sadeghi, B.; Garmaroudi, F.S.; Hashemi, M.; Nezhad, H.R.; Nasrollahi, A.; Ardalan, S.; Ardalan, S. Comparison of the anti-bacterial activity on the nanosilver shapes: Nanoparticles, nanorods and nanoplates, *Adv. Powder Technol.* 23, 2012, 22–26.

[165] Pal, S.; Tak, Y.K.; Song, J.M. Does the antibacterial activity of silver nanoparticles depend on the shape of the nanoparticle? A study of the gram-negative bacterium Escherichia coli. *Appl. Environ. Microbiol.* 73, 2007,

1712–1720.

[166] Choi, O.; Hu, Z. Size dependent and reactive oxygen species related nanosilver toxicity to nitrifying bacteria. *Environ. Sci. Technol.*, 42, 2008, 4583–4588.

[167] Sotiriou, G.A.; Pratsinis, S.E. Antibacterial activity of nanosilver ions and particles. Environ. Sci. Technol., 44, 2010, 5649–5654.

[168] Morones, J.R.; Elechiguerra, J.L.; Camacho, A.; Holt, K.; Kouri, J.B.; Ramirez, J.T.; Yacaman, M.J. The bactericidal effect of silver nanoparticles. Nanotechnology, 16, 2005, 2346–2353.

[169] E. Ataman, M. P. Andersson, M. Ceccato, N. Bovet, and S. L. S. Stipp, Functional Group Adsorption on Calcite: I. Oxygen Containing and Nonpolar Organic Molecules, *The Journal of Physical Chemistry*, 120 (30), 2016, 16586-16596.

[170] Amy Preszler Prince, Paul D. Kleiber, Vicki H. Grassian, Mark A. Young, Reactive uptake of acetic acid on calcite and nitric acid reacted calcite aerosol in an environmental reaction chamber,*Phys. Chem. Chem. Phys.*, 10, 2008, 142-152.

[171] S. R. Tong, L. Y. Wu, M. F. Ge, W. G. Wang, and Z. F. Pu, Heterogeneous chemistry of monocarboxylic acids on α-Al2O3 at ambient condition, *Atmos. Chem. Phys. Discuss*., 10, 2010, 3937–3974.

[172] Ning Yang, Narcisse T. Tsona, Shumin Cheng, Siyang Li, Li Xu, YifengWang, Lingyan Wu, Lin Du, Competitive reactions of SO_2 and acetic acid on α-Al_2O_3 and C.C. particles, *Science of the Total Environment* 699, 2020, 134362.

[173] Shen Zhang, Jincheng Xing, Jihong Ling, Huanhuan Yang, Experimental study on performance and influencing factors of chitosan-based nonwoven on gaseous HCHO removal, *Building and Environment*, 190, 2021, 107565.

[174] T. Prosek, M. Kouril, M. Dubus, M. Taube, V. Hubert, B. Scheffel, Y. Degres, M. Jouannic, D. Thierry, Real-time monitoring of indoor air

corrosivity in cultural heritage institutions with metallic electrical resistance sensors, *Studies in Conservation*, 58:2, 2013, 117-128.

[175] Magnus Johnson and Christofer Leygraf, Atmospheric Corrosion of Zinc by Organic Constituents: III. An Infrared Reflection-Absorption Spectroscopy Study of the Influence of Formic Acid, *J. Electrochem. Soc.* 153, 2006, B547.

[176] J. Hedberg, S. Baldelli, C. Leygraf, *Journal of The Electrochemical Society*, 157 (10), 2010, C363-C373.

[177] R. Wiesinger, S. Schnöller, H. Hutter, M. Schreiner, Ch. Kleber, About the Formation of Basic Silver Carbonate on Silver Surfaces – An In Situ IRRAS Study, *The Open Corrosion Journal*, 2, 2009, 96-104

[178] P. Uznanski, J. Zakrzewska, F. Favier, Synthesis and characterization of silver nanoparticles from (bis)alkylamine silver carboxylate precursors, *J. Nanopart. Res.*, 19, 2017, 121.

[179] Jean Tétreault, The Evolution of Specifications for Limiting Pollutants in Museums and Archives, *J.CAC*, 43, 2018, 21–37.

[180] BS 5454, Recommendations for the Storage and Exhibition of Archival Documents, *London: British Standards Institution*, 1977.

[181] Thomson, Garry, The Museum Environment, *London: Butterworths*, 1978.

[182] NBS 1983, Johnson, W.B., W.P. Lull, C.A. Madson et al., Environmental Control for Archival Record Storage, Washington, DC: National Bureau of Standards.

[183] NTC 1986, National Research Council, Preservation of Historical Records, Washington, DC: National Academy Press.

[184] BS 5454, Recommendations for the Storage and 198948 Exhibition of Archival Documents, London: 200049 British Standards Institution.

[185] NISO TR01, Environmental Guidelines for the Storage of Paper Records, Bethesda, MD: National Information Standards Organization Press, 1995.

[186] United Nations Educational, Scientific and Cultural Organization (UNESCO), 1998, Boston, G. (ed.), Safeguarding the Documentary Heritage: A Guide to Standards, Recommended Practices, and Reference Literature Related to the Preservation of Documents of All Kinds, Milton Keynes, UK: UNESCO."

[187] NARA 1571, Archival Storage Standards, Washington, DC: National Archives and Records Administration.

[188] PAS 198, Specification for Managing Environmental Conditions for Cultural Collections, London: British Standards Institution, 2012.

[189] T. Furuike, D. Komoto, H. Hashimoto, H. Tamura, *International Journal of Biological Macromolecules* 104, 2017, 1620–1625.

[190] S. Prati, E. Joseph, G. Sciutto, R. Mazzeo, New Advances in the Application of FTIR Microscopy and Spectroscopy for the Characterization of Artistic Materials, A*ccounts of Chemical Research,* Vol. 43, 2010, 792-801.

[191] l. Cartechini, C. Miliani, B.G. Brunetti, A. Sgamellotti, C. Altavilla, E. Ciliberto, F. D'Acapito,, X-ray absorption investigations of copper resinate blackening in a XV century Italian painting, Appl. Phys. A 92, 2008, 243–250.